

# THE FEBRUARY 1969 EAST RIFT ERUPTION OF KILAUEA VOLCANO HAWAII

GEOLOGICAL SURVEY  
PROFESSIONAL PAPER 891





# The February 1969 East Rift Eruption of Kilauea Volcano, Hawaii

By DONALD A. SWANSON, DALLAS B. JACKSON, ROBERT Y. KOYANAGI, and  
THOMAS L. WRIGHT

---

GEOLOGICAL SURVEY PROFESSIONAL PAPER 891



**UNITED STATES DEPARTMENT OF THE INTERIOR**

**THOMAS S. KLEPPE**, *Secretary*

**GEOLOGICAL SURVEY**

**V. E. McKelvey**, *Director*

---

Library of Congress Cataloging in Publication Data

Swanson, Donald A.

The February 1969 east rift eruption of Kilauea Volcano, Hawaii.

(Geological Survey Professional Paper 891)

Bibliography: p. 29-30.

Supt. of Docs. No.: I 19.16:891

1. Kilauea. I. Swanson, Donald A. II. Series: United States Geological Survey Professional Paper 891

QE23.K5F4

551.2'1'099691

75-619084

---

For sale by the Superintendent of Documents, U.S. Government Printing Office  
Washington, D.C. 20402

Stock Number 024-001-02761-5

## CONTENTS

	Page		Page
Abstract .....	1	Ground deformation in the summit area—continued	
Introduction .....	1	Horizontal deformation .....	19
Acknowledgments .....	1	Ground deformation in the eruption area .....	19
Preeruption events .....	2	Ground cracking .....	19
Swelling of the summit region .....	2	Horizontal deformation .....	20
Deformation of the east rift zone .....	6	Vertical deformation .....	21
Seismic activity in the summit region .....	6	Depth to summit magma reservoir .....	22
Seismic activity on the east rift zone and south flank .....	6	Elastic and plastic pseudo-chamber models .....	22
Narrative of the eruption .....	8	Three dimensional displacement method .....	23
Petrography and chemistry of the lava .....	12	Discussion and speculation .....	23
Seismic activity during the eruption .....	14	Eruption prediction by using deformation data .....	25
Ground deformation in the summit area .....	16	Makaopuhi magma reservoir .....	26
Tilt .....	16	Nature of magma conduit between summit and eruption site .....	28
Vertical displacement .....	18	References cited .....	29

## ILLUSTRATIONS

		Page
PLATE	1. Geologic map of products of the August and October 1968 and February 1969 east rift eruptions .....	In pocket
FIGURE	1. Index map of summit and upper east rift zone of Kilauea showing area of lava erupted in February 1969 and fissures of August and October 1968 eruptions .....	2
	2. Graph showing seismic activity, ground tilt, and dilatational strain between October 5, 1968 and March 31, 1969 .....	3
	3. Map showing ground tilt at Uwekahuna for interval between October 22, 1968 and February 22, 1969 .....	4
	4. Maps showing ground tilt and vertical displacement before the February 1969 eruption .....	4
	5. Maps showing horizontal displacement and dilatational strain before the February 1969 eruption .....	5
	6. Maps showing epicenters and magnitudes of earthquakes before the February 1969 eruption .....	7
	7. Photograph of Alae Crater on March 21, 1969 .....	8
	8. Diagram showing time and duration of eruptive activity .....	9
9-15.	Photographs:	
	9. Aerial view of Makaopuhi Crater, March 1969 .....	10
	10. Lava drapery on walls of Makaopuhi Crater .....	10
	11. Aerial view of aa flow along Chain of Craters Road .....	11
	12. Two-tier lava cascade into Alae Crater .....	11
	13. Opening of and initiation of fountaining from a fissure across Chain of Craters Road .....	12
	14. Lobes of aa in Napau Crater .....	13
	15. Aerial view showing row of spatter cones west of Alae Crater .....	14
	16. Graph showing summary of ground tilt and seismicity during eruption .....	15
	17. Map showing epicenters and magnitudes of shallow earthquakes, February 22 to February 28, 1969 .....	15
	18. Graph showing tilt records at Uwekahuna and Outlet between February 21 and March 2, 1969 .....	16
	19. Maps showing ground tilt changes at Uwekahuna and Outlet between February 22 and March 2, 1969 .....	17
	20. Map showing ground tilt and vertical displacement between February 4-5 and March 3-5, 1969 .....	18
	21. Map showing horizontal displacement and dilatational strain near summit and upper east rift zone between February 11-13 and February 24-27, 1969 .....	20
	22. Map showing length changes of five geodimeter lines between February 23 and 25, 1969 .....	21
	23. Photograph of new opening of old crack across Chain of Craters Road .....	21
	24. Photograph of master crack bounding slump block at Alae Crater .....	22
	25. Graphs of ground-deformation models .....	24
	26. Diagram showing range of calculated source depths of figure 25 .....	25
	27. Graph showing horizontal and vertical field data compared with curves for vertical-plug model .....	26
	28. Graph showing source depths derived from three-dimensional displacements .....	26
	29. Diagram of cumulative extension for five geodimeter lines between mid-October 1968 and mid-May 1969 .....	27

## TABLES

TABLE		Page
1.	The four largest south flank earthquakes between the October 1968 and February 1969 eruptions, Kilauea Volcano	8
2.	Chemical analyses of lava from the February 1969 eruption of Kilauea Volcano	13
3.	Modal analyses of lava from the February 1969 eruption of Kilauea Volcano	13
4.	Estimated maximum eruption temperatures of February 1969 lava, Kilauea Volcano	14
5.	Displacements of survey stations and depths to pressure source (magma reservoir) beneath Kilauea Caldera before and during February eruption	25
6.	Cumulative extension of distances in summit strain monitor for two periods of inflation, Kilauea Volcano	27

## METRIC-ENGLISH EQUIVALENTS

Metric unit	English equivalent	Metric unit	English equivalent
<b>Length</b>		<b>Specific combinations—Continued</b>	
millimetre (mm)	= 0.03937 inch (in)	litre per second (l/s)	= .0353 cubic foot per second
metre (m)	= 3.28 feet (ft)	cubic metre per second per square kilometre [(m <sup>3</sup> /s)/km <sup>2</sup> ]	= 91.47 cubic feet per second per square mile [(ft <sup>3</sup> /s)/mi <sup>2</sup> ]
kilometre (km)	= .62 mile (mi)	metre per day (m/d)	= 3.28 feet per day (hydraulic conductivity) (ft/d)
<b>Area</b>		metre per kilometre (m/km)	= 5.28 feet per mile (ft/mi)
square metre (m <sup>2</sup> )	= 10.76 square feet (ft <sup>2</sup> )	kilometre per hour (km/h)	= .9113 foot per second (ft/s)
square kilometre (km <sup>2</sup> )	= .386 square mile (mi <sup>2</sup> )	metre per second (m/s)	= 3.28 feet per second
hectare (ha)	= 2.47 acres	metre squared per day (m <sup>2</sup> /d)	= 10.764 feet squared per day (ft <sup>2</sup> /d) (transmissivity)
<b>Volume</b>		cubic metre per second (m <sup>3</sup> /s)	= 22.826 million gallons per day (Mgal/d)
cubic centimetre (cm <sup>3</sup> )	= 0.061 cubic inch (in <sup>3</sup> )	cubic metre per minute (m <sup>3</sup> /min)	= 264.2 gallons per minute (gal/min)
litre (l)	= 61.03 cubic inches	litre per second (l/s)	= 15.85 gallons per minute
cubic metre (m <sup>3</sup> )	= 35.31 cubic feet (ft <sup>3</sup> )	litre per second per metre [(l/s)/m]	= 4.83 gallons per minute per foot [(gal/min)/ft]
cubic metre	= .00081 acre-foot (acre-ft)	kilometre per hour (km/h)	= .62 mile per hour (mi/h)
cubic hectometre (hm <sup>3</sup> )	= 810.7 acre-feet	metre per second (m/s)	= 2.237 miles per hour
litre	= 2.113 pints (pt)	gram per cubic centimetre (g/cm <sup>3</sup> )	= 62.43 pounds per cubic foot (lb/ft <sup>3</sup> )
litre	= 1.06 quarts (qt)	gram per square centimetre (g/cm <sup>2</sup> )	= 2.048 pounds per square foot (lb/ft <sup>2</sup> )
litre	= .26 gallon (gal)	gram per square centimetre	= .0142 pound per square inch (lb/in <sup>2</sup> )
cubic metre	= .00026 million gallons (Mgal or 10 <sup>6</sup> gal)	<b>Temperature</b>	
cubic metre	= 6.290 barrels (bbl) (1 bbl=42 gal)	degree Celsius (°C)	= 1.8 degrees Fahrenheit (°F)
<b>Weight</b>		degrees Celsius (temperature)	= [(1.8 × °C) + 32] degrees Fahrenheit
gram (g)	= 0.035 ounce, avoirdupois (oz avdp)		
gram	= .0022 pound, avoirdupois (lb avdp)		
tonne (t)	= 1.1 tons, short (2,000 lb)		
tonne	= .98 ton, long (2,240 lb)		
<b>Specific combinations</b>			
kilogram per square centimetre (kg/cm <sup>2</sup> )	= 0.96 atmosphere (atm)		
kilogram per square centimetre	= .98 bar (0.9869 atm)		
cubic metre per second (m <sup>3</sup> /s)	= 35.3 cubic feet per second (ft <sup>3</sup> /s)		

# THE FEBRUARY 1969 EAST RIFT ERUPTION OF KILAUEA VOLCANO, HAWAII

BY DONALD A. SWANSON, DALLAS B. JACKSON, ROBERT Y. KOYANAGI,  
and THOMAS L. WRIGHT

## ABSTRACT

Between February 22 and 28, 1969, about  $20 \times 10^6 \text{ m}^3$  of basaltic lava covered more than  $6 \text{ km}^2$  of the upper east rift zone of Kilauea Volcano, probably the largest recorded eruption on the upper rift to that time. The eruption broke out along a discontinuous, 11-km-long fissure zone extending downrift from near Aloi Crater. A 70-m-deep lava lake formed in Alae Crater, near the site of the most prolonged activity. The lava is olivine-poor tholeiite; its hybrid chemistry can be explained by mixing of magma of 1967–68 summit vintage with that erupted during the early part of the 1969–71 Mauna Ulu eruption and with lesser amounts of differentiated magma like that erupted in October 1968. The eruption followed a 4-month-long period of summit and east rift tumescence and was accompanied by moderate summit deflation and severe uplift and dilation near the eruption site. The centers of horizontal and vertical deformation in the summit area migrated laterally before and during the eruption in response to the filling and emptying of a complex reservoir system. Comparison of depths to the summit reservoir derived from five theoretical models and a graphic approach shows poor agreement, although all agree on depths of less than 5 km. The pattern of seismicity, timing of deformation and eruptive events, and chemistry of the lava imply the presence of a shallow magma reservoir on the east rift near Makaopuhi Crater. Seismic data suggest the existence of a nearly unobstructed magma conduit within the rift zone long before the eruption. Dikes that fed magma to the surface issued from this conduit, not directly from the summit reservoir.

## INTRODUCTION

For the third time since the end of the 1967–68 summit eruption in July 1968 (Kinoshita and others, 1969), Kilauea Volcano erupted along its east rift zone, February 22 to 28, 1969. The pattern of repeated flank eruptions, with no intervening summit eruption, characterized much of Kilauea's volcanic activity during the 1960's (Moore and Koyanagi, 1969; Peck and others, 1966; Wright and others, 1968; Fiske and Koyanagi, 1968; Jackson and others, 1975; Swanson and others, 1971); this is a departure from the pattern of the preceding decade, when each flank eruption was preceded by a summit eruption.

The February 1969 eruption took place along a discontinuous, 11-km-long line of fissures from about 0.5 km south of Aloi Crater to 4 km east-northeast of Napau Crater (pl. 1; fig. 1). Most activity was concentrated between Alae Crater and the prehistoric lava shield,

Kane Nui o Hamo, where the new fissures opened very close to those of the December 1962 and December 1965 eruptions (Moore and Krivoy, 1964; Fiske and Koyanagi, 1968). Lava eventually pooled to form a lake 70 m deep in Alae Crater, and three large spatter cones as high as 35 m were formed between Alae and Kane Nui o Hamo. About  $20 \times 10^6 \text{ m}^3$  of lava was erupted in what at the time was probably the largest eruption on the upper east rift zone during historic time (since 1750); the 1969–71 Mauna Ulu eruption (Swanson and others, 1971) subsequently far surpassed this volume. Most of the flows and cones formed during the February 1969 eruption were buried by younger lava within a year, and Alae Crater, the site of much of the February activity, was filled to overflowing in October 1969 (Swanson and others, 1972). These changes provide mute testimony to the transitory nature of landscapes on active volcanoes.

The geodetic networks for measuring ground displacement at Kilauea were expanded and occupied shortly before the eruption began, and a new program of frequent horizontal strain measurements across Kilauea Caldera was instituted in late October 1968, following the October 7–22 flank eruption. Data from these surveys, combined with daily tilt readings and extensive seismic coverage, provide an unusually complete record of structural events before, during, and after the eruption.

## ACKNOWLEDGMENTS

We thank the resident staff of the Hawaiian Volcano Observatory and its former Scientist-in-Charge, H. A. Powers, for skillful field and laboratory assistance. The Civil Air Patrol based in Hilo graciously provided aerial reconnaissance during the eruption. W. A. Duffield, later on the staff of the Observatory, contributed energetic support during late stages of the eruption. National Park Service personnel made numerous helpful observations and gave posteruption logistic aid. The paper benefits from the reviews of our colleagues, J. P. Lockwood and D. W. Peterson.

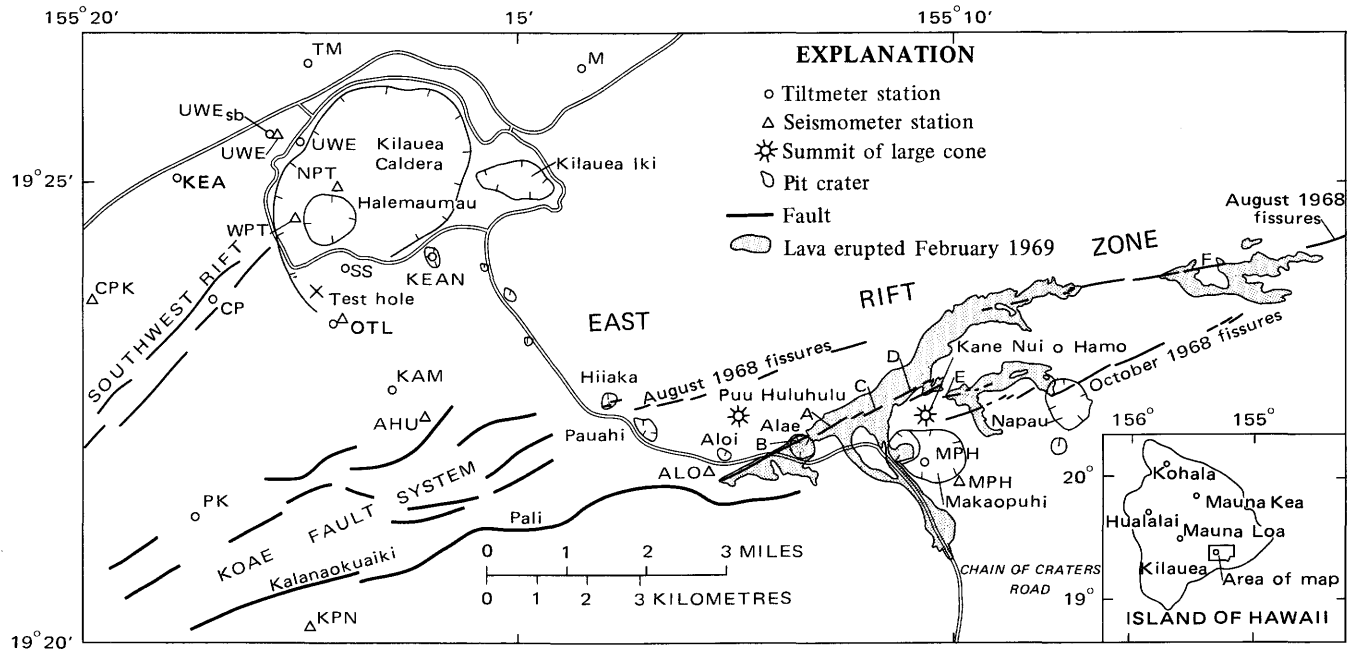


FIGURE 1.—Index map of summit and upper east rift zone of Kilauea showing area of lava erupted in February 1969, the western fissures of the August 1968 eruption, and the fissures of the October 1968 eruption. Specific vent areas indicated by letters. Outline of February 1969 lava erupted west of vent D approximate; flows from the 1969–71 Mauna Ulu eruption covered February 1969 flows before they were mapped. Additional seismometer stations not shown on map used for locating and recording earthquakes are given by Koyanagi, Takeguchi, and Kinoshita (1970). Kalanaokuaihi Pali is a north-facing fault scarp along the south boundary of the Koae

fault system. Summits of five volcanoes that make up the island of Hawaii shown in inset. Seismometer stations: OTL, Outlet; UWE, Uwekahuna; NPT, North Pit; WPT, West Pit; AHU, Ahua; KPN, Kipuka Nene; ALO, Aloi; MPH, Makaopuhi; CPK, Cone Peak. Tiltmeter stations: KEA, Keamoku; UWE<sub>sb</sub>, Uwekahuna short-base; UWE, Uwekahuna long-base; SS, Sand Spit; KEAN, Keanakakoi; OTL, Outlet; KAM, Ahua; PK, Puu Koa; MPH, Makaopuhi; TM, Tree Molds; M, Mehana; CP, Cone Peak. Location of 1.26 km test hole drilled in 1973 also shown.

## PREERUPTION EVENTS

### SWELLING OF THE SUMMIT REGION

The swelling of the summit region of Kilauea before eruption has been documented by measurement of ground deformation over the past 20 years. The swelling is presumed to reflect the filling and expansion of a shallow, complex magma reservoir system. The February 1969 eruption, which followed a period of prolonged inflation that began even before the October 1968 flank eruption had ended as magma replenished the reservoir system faster than it erupted (Jackson and others, 1975), fits this typical pattern. This swelling was detected and traced by tiltmeters, leveling surveys, and horizontal-distance measurements with a Model 6 geodimeter using the techniques described by Kinoshita, Swanson, and Jackson (1974).

Daily readings of the short-base water-tube tiltmeters in Uwekahuna vault show the swelling most clearly (fig. 2A). By October 22, the last day of the October 1968 eruption, the summit region had already begun to reinflate at a rate of about  $0.8 \mu\text{rad}$  per day. Between December 1 and 11, a small episode of summit deflation occurred; then swelling resumed once more at

a steady but reduced rate until February 1, 1969. Between January 25 and February 15, there was a small reversal of the east-west component of tilt, probably indicating slight deflation of the northern part of the caldera east of Uwekahuna. This event was immediately followed by rapid summit swelling at a rate of about  $4 \mu\text{rad}$  per day that continued into the early morning of February 22, when summit deflation immediately preceding the flank eruption began. The last burst of swelling coincides with a sharp increase in the daily count of shallow summit earthquakes (fig. 2C) and may record the failure of the reservoir wallrock just before magma was released into the east rift conduit system.

A plot of cumulative dilatation for one of the triangles in the geodimeter network shows that the summit region was expanding laterally as well as tilting (fig. 2B). Dilatation, as used herein, is the change in area of a surveyed triangle divided by the original area and is presented in units of  $10^{-5}$  (parts per hundred thousand) or  $10^{-6}$  (parts per million). The nearly equilateral triangle shown in figure 2, which spans part of Kilauea Caldera, increased in area by about  $450 \text{ m}^2$ , indicating a dilatational strain of about  $11.5 \times 10^{-5}$  between October

11, 1968 and February 4, 1969. The area of the triangle then decreased slightly between February 4 and 11, consistent with the accompanying tilt reversal at Uwekahuna vault. The rate of change, about  $10^{-6}$  per day, was remarkably linear throughout most of period of swelling despite the large size of the survey triangle and the complex pattern of tilting. The maximum dilatation before the February eruption was  $18 \times 10^{-5}$  relative to an arbitrary zero datum established the first time the triangle was measured in July 1966 during a period of prolonged summit inflation (Fiske and Kinoshita, 1969, fig. 2) when the summit region was strained to an unknown degree.

From a plot of vectors from the Uwekahuna water-tube tilt record for selected intervals (fig. 3), we can infer that the center of summit swelling migrated 2-3 km during the preeruption period, oscillating in a north-south direction before reaching its final position south of Halemaumau just before the eruption. Such a migration, usually in a net southerly sense, has been typical of recent inflation and deflation episodes at Kilauea (Fiske and Kinoshita, 1969; Jackson and others, 1975). The period for which vectors 1 and 2 (fig. 3) were calculated nearly coincides with the leveling period that defines uplift A, and the swing of the vectors suggests that swelling migrated slightly northward within uplift A during this interval. The pattern of swelling is more complex for tilt intervals 3 through 8, with two episodes of deflation during intervals 3 and 7 and a general northerly migration of the center of swelling during intervals 4, 5, and 6. The center of tilting moved sharply southward during interval 8, immediately before the flank eruption, suggesting that the final surge of swelling was in uplift B south of Halemaumau. The resultant of vectors for intervals 3 through 8 shows that the net tilt from January 1 to February 22 was up to the south along an azimuth passing directly through uplift B.

Leveling, tilt, and trilateration surveys of the entire summit region conducted in October and November-

December 1968 and early February 1969 further document the overall southerly migration of the center of inflation and define the shape and dimensions of the uplift (figs. 4 and 5). The tilt and leveling surveys were conducted concurrently; their results (fig. 4) are in good agreement, especially if an empirical clockwise adjustment of  $20^\circ$ , consistently found to reduce the scatter in the data, is made to the azimuth of the Uwekahuna short-base tilt vector. The tilt and leveling data indicate

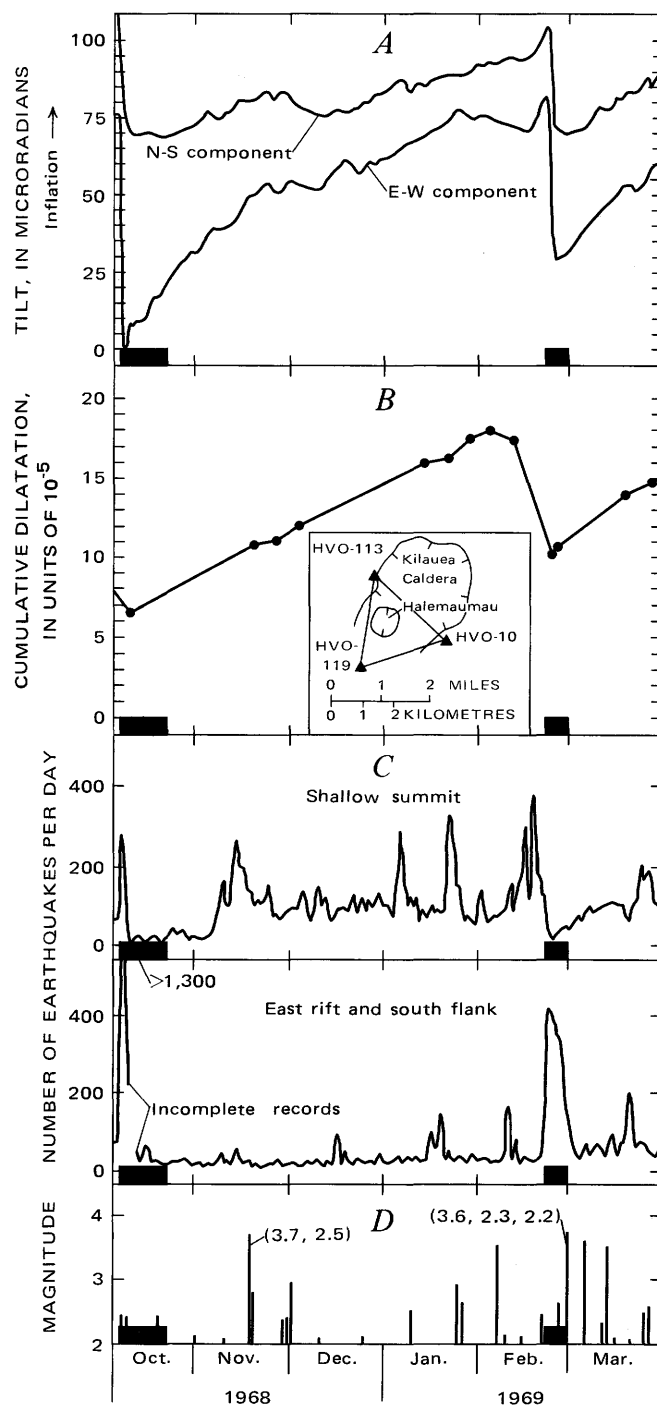


FIGURE 2.—Summary of seismic activity, ground tilt, and dilatational strain at Kilauea Volcano between October 5, 1968 and March 31, 1969. *A*, Ground tilt. Daily readings are from east-west and north-south components of short-base, water-tube tiltmeter in Uwekahuna vault,  $UWE_{sb}$  (fig. 1). *B*, Cumulative dilatation (the change in area of the survey triangle divided by the original area) plotted relative to arbitrary zero datum established in July 1966. *C*, Earthquake counts. Shallow summit earthquakes recorded by the North Pit (NPT) seismograph; east rift zone and south flank earthquakes by the Makaopuhi (MPH) and Aloi (ALO) seismographs (fig. 1). The numbers of earthquakes counted during the February 1969 eruption are minimum figures, because intense harmonic tremor obscured many small earthquakes. *D*, Deep summit earthquakes (15-35 km focal depth) with Richter magnitude greater than 2. Solid bars, time and duration of October 1968 and February 1969 eruptions.

that the center of swelling migrated about 2 km southward some time between late November and early February (fig. 4B), consistent with the more detailed record of tilt at Uwekahuna (compare vectors 2 and 4, fig. 3). The maximum measured uplift in the summit area amounted to 5.7 cm for the first leveling interval and 8.6 cm for the second. The datum point for the two leveling surveys is arbitrary and may have been uplifted an unknown amount, although probably less than 2 cm, judged by more extensive surveys in August 1968 and February 1969.

The zone of subsidence in the south part of the caldera during the October to November survey period (fig. 4A) is not consistent with overall summit uplift. The October survey was conducted near the conclusion of an episode of marked summit deflation (Jackson and others, 1975), and local subsidence in the south caldera area probably continued after inflation resumed

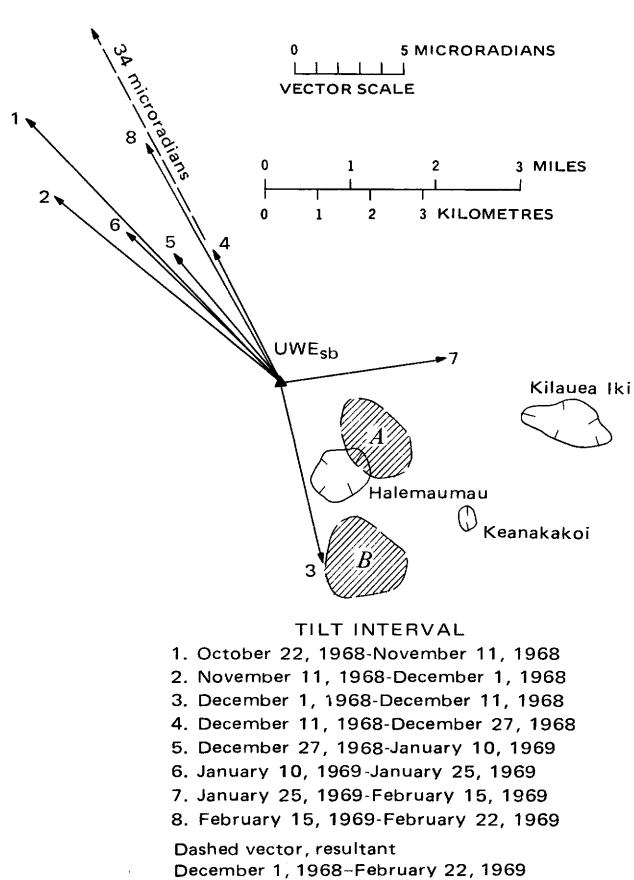


FIGURE 3.—Ground tilt (vectors) for selected intervals between October 22, 1968 and February 22, 1969. Vectors plotted by using the north-south and east-west Uwekahuna short-base water-tube tiltmeters. All vectors have been adjusted by a 20° clockwise rotation, an empirical adjustment that appears valid during times of rapid summit deflation. A, center of 50 mm uplift between early October and late November 1968, B, center of 80 mm uplift between late November and early February 1969, as determined by leveling (fig. 4).

elsewhere. This local subsidence was still recognizable at the time of the next survey in late November.

Each trilateration survey was conducted several days after the corresponding leveling and tilt surveys. As the

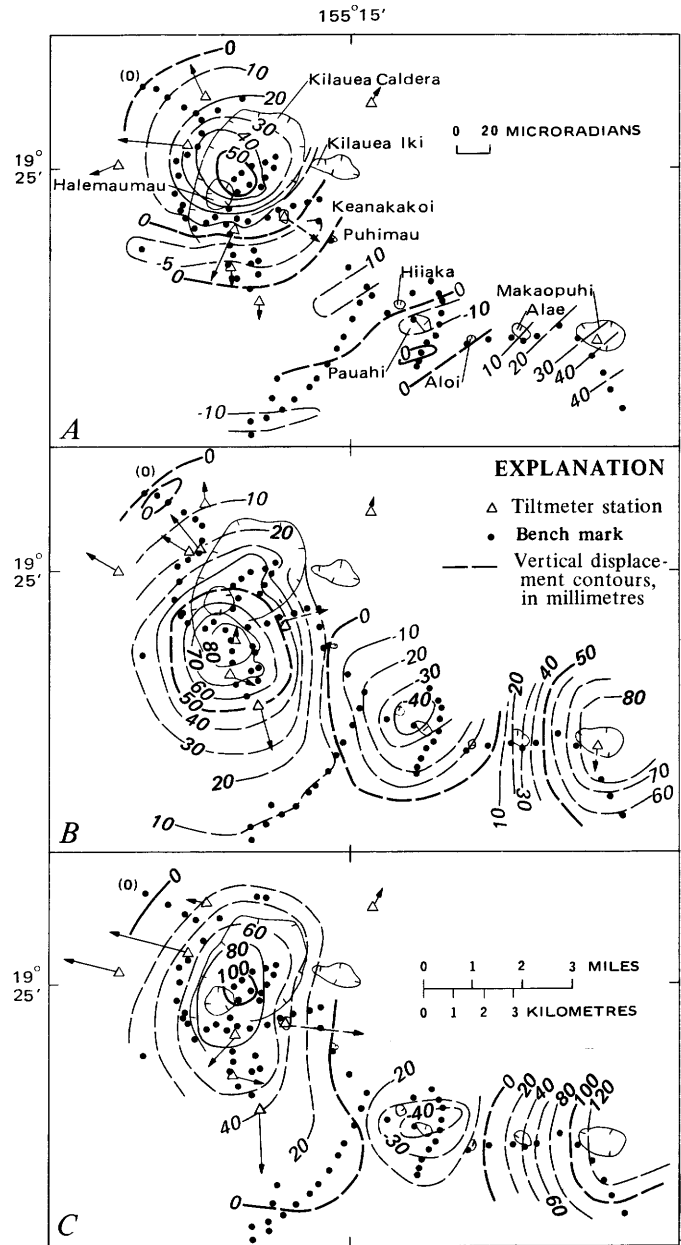


FIGURE 4.—Ground tilt (vectors) and vertical displacement (contours) for three periods before the February 1969 eruption. A, October 9–10 to November 15–26, 1968. B, November 25–26, 1968 to February 4–5, 1969. C, Summary of periods in A and B. Bench marks used in leveling surveys are relative to arbitrary datum point, the northwesternmost bench mark (O). Dashed tilt vectors obtained by spirit-level tilting (Kinoshita and others, 1974); all other tilting was by conventional water-tube methods (Eaton, 1959; Kinoshita and others, 1974). Dashed contours, uncertain.

summit area was undergoing continuous deformation during this time, the trilateration data are not strictly comparable to the other data. Nonetheless, the horizontal displacements and dilation also show a southerly shift in the center of uplift (fig. 5A, B). In addition, they define a somewhat more westerly center than the tilt and leveling data for the second survey interval, perhaps indicating a net westward migration between the times of the trilateration and level-tilt surveys, such as that in 1967 documented by Fiske and Kinoshita (1969). Both the horizontal and vertical data (figs. 4B and 5B) suggest that a subsidiary center of uplift formed about 1 km northwest of station HVO-114 between early December and early February; this location is within the caldera as defined by circumferential faults but south of the topographic depression that indents Kilauea's summit area.

The azimuth of horizontal displacement at Cone Peak disagrees with the overall pattern by suggesting a more southerly deformation center, especially during the December-February interval. Cone Peak is bounded by gaping cracks of the southwest rift zone and typically shows displacements that tend to be perpendicular to the cracks (Hawaiian Volcano Observatory, unpub. data, 1971). This relation suggests that the cracks markedly affect the local strain field.

The summary maps (figs. 4C and 5C) show the net deformation during the preeruption period of inflation. The center of net uplift was located near the northeast rim of Halemaumau Crater, and the center of horizontal expansion was located about 1 km away, near the south edge of Halemaumau. We do not know if this difference in location is real or if it is due to the fact that the trilateration survey did not exactly coincide in time with the tilt and level surveys. Maximum vertical displacement in the summit area was about 11 cm relative to a bench mark 4.5 km northwest of the center of uplift, and the volume of uplift was more than  $2.4 \times 10^6 \text{ m}^3$ . The

maximum measured horizontal displacement was about 16 cm, and the area of the summit region increased by more than  $2 \times 10^3 \text{ m}^2$ .

These summary maps are deceptively simple, as shown by comparison with the maps of the shorter in-

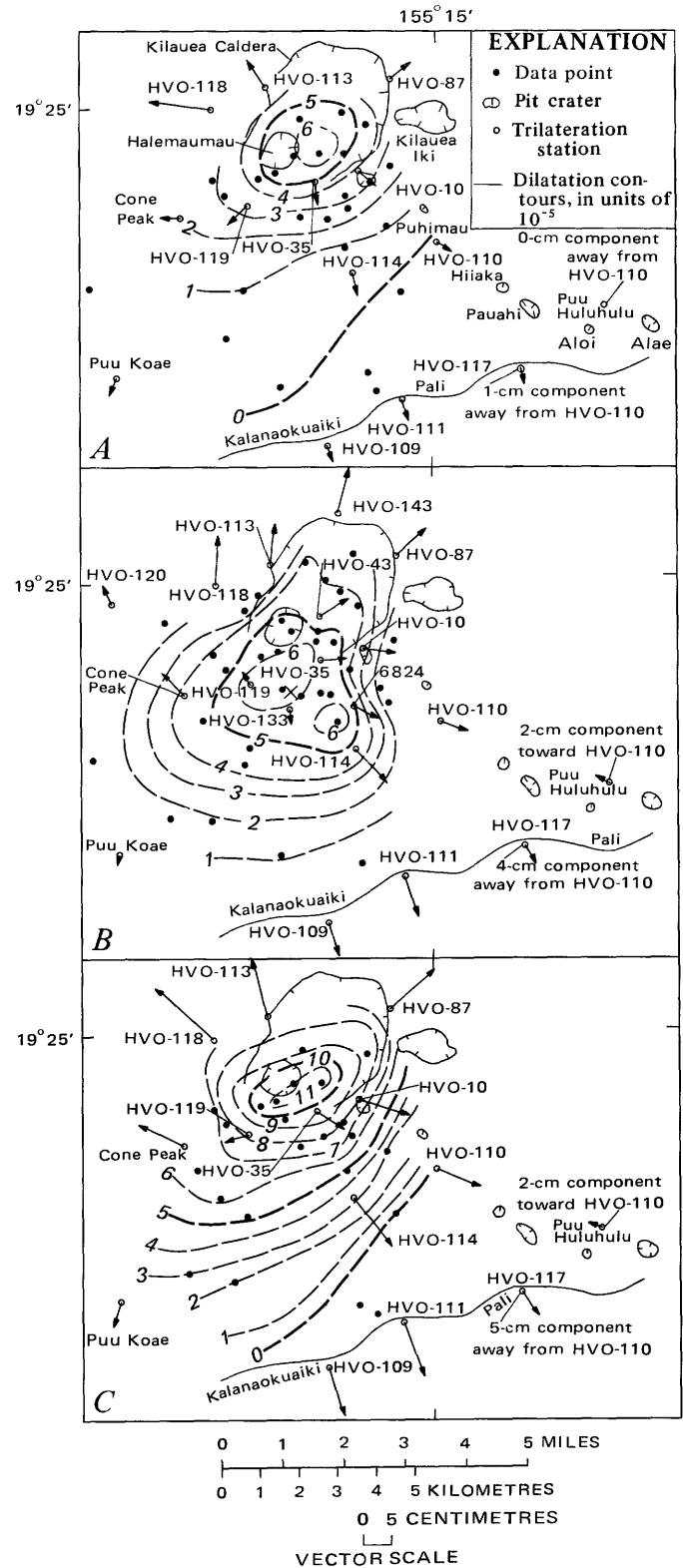


FIGURE 5. Horizontal displacement (vectors) and dilatational strain (contours) in Kilauea summit area for three periods before the February 1969 eruption. A, October 10-15 to December 2-10, 1968. B, December 2-10, 1968 to February 11-13, 1969. C, Summary of A and B. Displacement, relative to a 4.4-km-long, north-northeast oriented baseline located between 5.3 and 8.5 km west-southwest of Puu Koaie, was determined by a least squares adjustment of trilateration data. Displacement determination of HVO-118 is less reliable owing to small angle of intersection. Components of displacement away from HVO-110 are indicated at Puu Huluhulu and HVO-117; as distances to these stations were measured from only one trilaterated station, HVO-110, complete vectors could not be calculated. Filled circles indicate center of gravity of each strain triangle for which dilatation was calculated, assuming homogeneous strain; dilatation values were plotted at the centers of gravity and then contoured (Kinoshita and others, 1974). Cross in B, center of deformation used in determination of three-dimensional displacements. Note the addition of five stations in B.

tervals, which more faithfully, but still incompletely, portray the complex nature of Kilauea's inflation. The migration of deformation centers clearly indicates that the swelling process cannot result from the filling of a single chamber in the usual sense of the term, as would be suggested by the summary maps alone. Rather, the reservoir system is most likely a complicated plexus of dikes and sills branching from near the top of the feeder conduit bringing magma up from the mantle. Some of these dikes and sills are apparently large enough to be subchambers, accepting magma during periods of swelling and expelling it during periods of deflation. It is in this sense that such terms as reservoir complex or reservoir system are used in this paper.

#### DEFORMATION OF THE EAST RIFT ZONE

During the preeruption period, the east rift zone underwent complex deformation (figs. 4 and 5) whose pattern and cause cannot be adequately defined. The area of initial eruptive activity in August 1968, near Hiiaka and Pauahi Craters (fig. 1), subsided throughout the fall and winter, apparently a continuation of a trend that began immediately after the August eruption (Jackson and others, 1975). Perhaps this subsidence is related to subsurface migration or cooling of stored August magma, or to continued adjustments along ground cracks that opened during the eruption.

An area of undetermined shape near Makaopuhi Crater was uplifted more than 12 cm between October and February. The center of uplift appears to have shifted from a location south of Makaopuhi for the October–November survey period (fig. 4A) to a site north of Makaopuhi for the November–February survey period (fig. 4B). The Makaopuhi area had been uplifted at least 21 cm between October 7 and 10, during the early stages of the October 1968 eruption (Jackson and others, 1975). As repeated levelings showed no significant uplift between October 10 and 25, we doubt that the subsequent uplift can be considered a continuation of uplift that accompanied the eruption. The post-October 25 uplift may record filling of a local magma reservoir, possibly one that eventually fed the February 1969 eruption. This possibility is examined in the "Discussion and Speculation" section.

#### SEISMIC ACTIVITY IN THE SUMMIT REGION

At the summit, only a few shallow earthquakes, most with focal depths of less than 5 km, were recorded during several weeks following the seismic crisis in the early part of the October 1968 eruption (Jackson and others, 1975). After the first week in November, summit seismicity increased, and the daily frequency of earthquakes fluctuated at moderate levels as the summit region became highly strained (fig. 2C). The seismic pattern changed in early January; flurries of shallow

quakes occurred on January 6, 22–23, and February 16 and 19. The swarm on January 22–23 was associated with an increased rate of summit dilation (fig. 2B); the two February flurries accompanied the brief period of very rapid inflation immediately preceding the eruption and were in retrospect premonitory warnings of the impending outbreak.

With continued high seismicity in February, many summit earthquakes were sufficiently strong (though mostly less than magnitude 2.0) to allow location of their hypocenters (Koyanagi and Endo, 1971). Most of these earthquakes originated less than 5 km beneath the southern part of Kilauea Caldera (fig. 6B), where swelling was concentrated (figs. 4B and 5B).

Long-period earthquakes, somewhat resembling short bursts of weak harmonic tremor, were especially frequent on October 28, November 7–8, January 11–12 and 23, and February 17–18. Precise focal determinations are unreliable because arrival times for these long-period events were poorly recorded. Rough estimates suggest that these quakes originated beneath the south caldera area at depths comparable to or somewhat deeper than the usual shallow summit earthquakes. The number of long-period events commonly increased during times of rapid ground deformation, suggesting an association with movement of magma and structural adjustments within the shallow reservoir complex.

Between November and February, a moderate number of deep (15–35 km) earthquakes occurred beneath the summit (fig. 2D). Hypocenters of these quakes define a narrow cylinder inclined vertically to steeply southward beneath the caldera (Koyanagi and Endo, 1971, fig. 5), appearing to outline the conduit system that transports magma from upper mantle sources or storage areas to shallow reservoirs within the volcano.

#### SEISMIC ACTIVITY ON THE EAST RIFT ZONE AND SOUTH FLANK

The daily number of south flank earthquakes decreased abruptly following the start of the October 1968 eruption and then leveled off at relatively high levels (fig. 2C). Brief periods of heightened seismicity became increasingly frequent between mid-November and February. Four large earthquakes that occurred between December 16 and February 9 beneath the south flank accounted for most of the strain release during the preeruption period (table 1).

The level of seismicity was especially high in an area 2 to 5 km south of the east rift zone between Hiiaka and Napau Craters (fig. 6A, B). Both the August and October 1968 eruptions had taken place along the adjacent segment of the rift zone and may have initiated long-term structural adjustments within the south flank (Koyanagi and others, 1972).

The daily number of earthquakes beneath the south

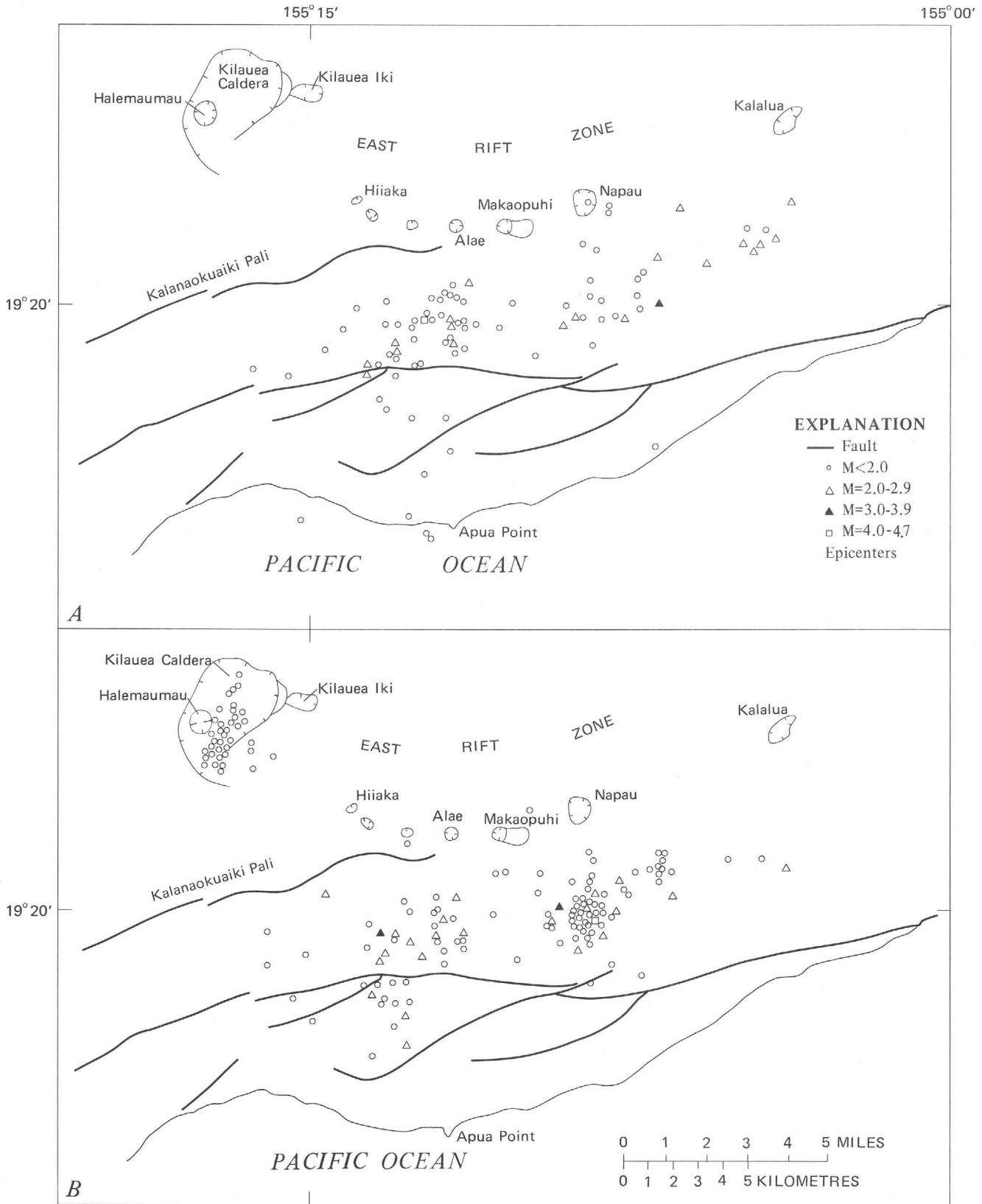


FIGURE 6.—Epicenters and magnitudes of earthquakes with focal depths of about 10 km or less that occurred in the summit and south flank areas for two time periods before the February 1969 eruption. A, November 1 to December 31, 1968. B, January 1 to February 21, 1969.

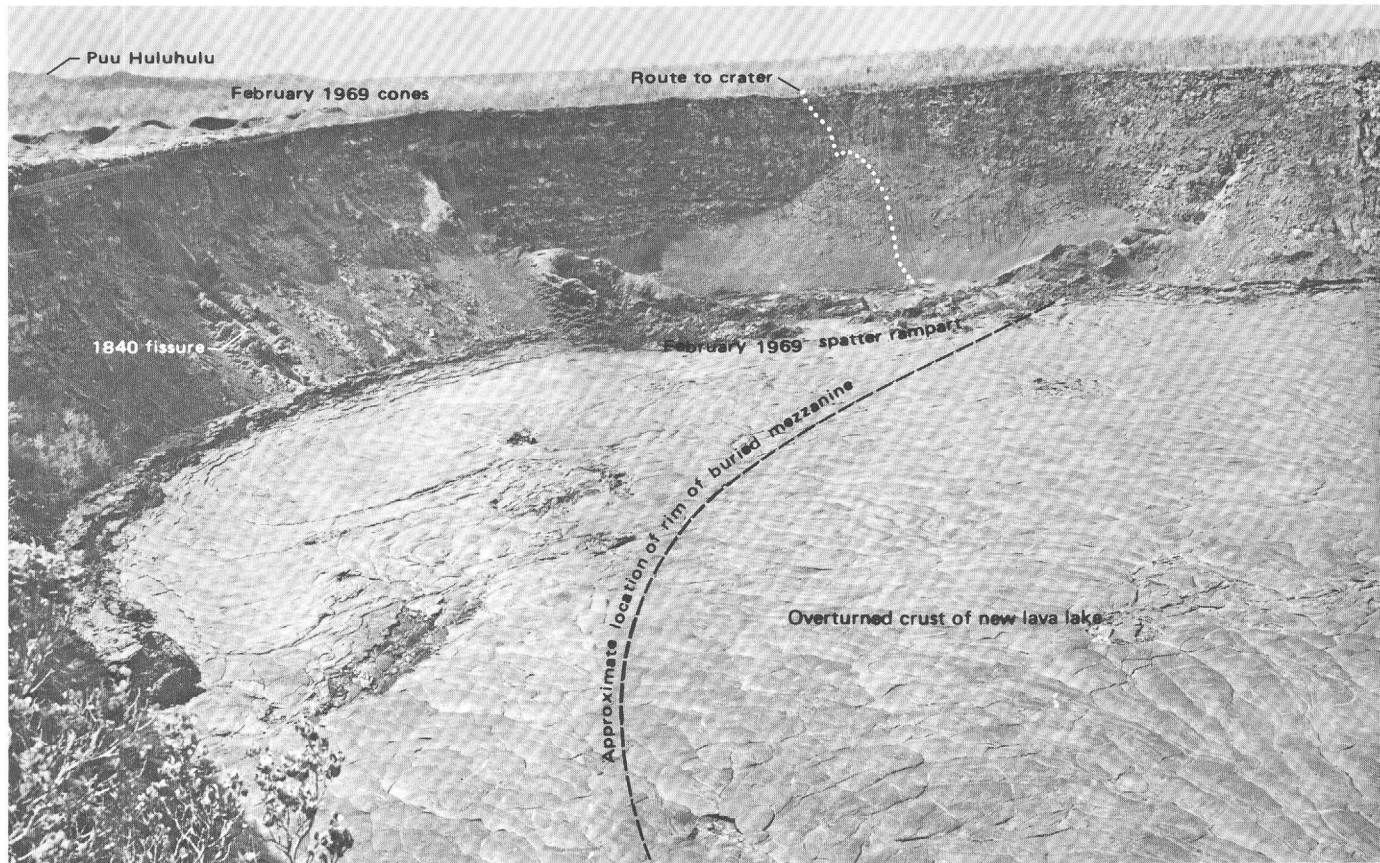


FIGURE 7.—February 1969 lava lake in Alae Crater viewed from south rim on March 21, 1969. A program of drilling through the crust into the lake was

flank gradually increased between November and February, particularly in the area south of Alae, Makaopuhi, and Napau Craters. This gradual increase may have been related to the uplift near Makaopuhi (fig. 4.) The overall heightened seismicity roughly correlates in time with the increase in summit seismicity, several intermittent bursts of south-flank earthquakes occurring 1 to 2 weeks after short-lived flurries of shallow caldera quakes.

By mid-February 1969, Kilauea was primed with magma. Not only the summit area but also the area

TABLE 1.—The four largest south flank earthquakes between the October 1968 and February 1969 eruptions, Kilauea Volcano

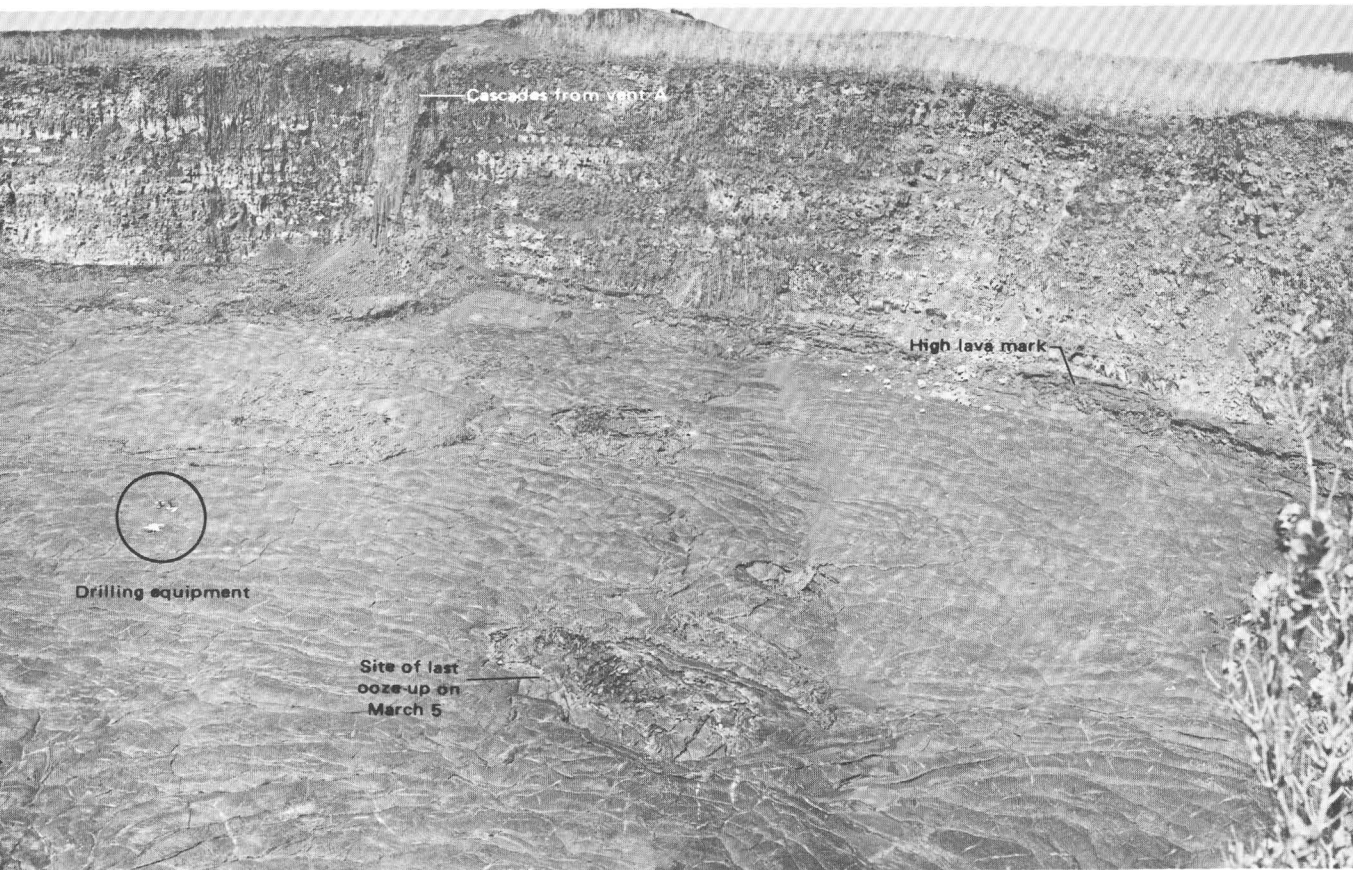
Date	h	Time <sup>1</sup> m s	Magnitude	Hypocenter	Remarks
Dec. 16	16	33 03.5	4.7	5 km SW of Makaopuhi at about 10-km depth	Felt islandwide; followed by about 150 aftershocks
Dec. 19	22	16 11.1	3.5	7 km SE of Makaopuhi at about 9-km depth	Felt in southeastern parts of the island; followed by about 50 aftershocks
Jan. 5	17	25 00.2	3.6	7 km SW of Makaopuhi at about 10-km depth	Felt in Kilauea summit area; followed by several aftershocks
Feb. 9	16	24 42.2	4.1	5 km SE of Makaopuhi at about 10-km depth	Felt islandwide; followed by about 170 aftershocks

<sup>1</sup>Hawaiian Standard Time.

near Makaopuhi Crater had been uplifted as a consequence of the influx and shallow storage of magma. Shallow earthquakes were frequent in or adjacent to both areas of uplift, and bursts of tremorlike long-period quakes had become increasingly common. The scene was set for an eruption.

#### NARRATIVE OF THE ERUPTION

A swarm of short bursts of harmonic tremor and small, shallow earthquakes within Kilauea's upper east rift zone began at about 0627, February 22. By 0900, the tremor was continuous at a steady amplitude, and an eruption was clearly imminent. Fifty minutes later fume was first sighted, and about this time excited tourists on the Chain of Craters Road reported low lava fountains at vent A, a fissure 300–500 m northeast of the rim of Alae Crater (figs. 1, 7, and 8). By 1030, a line of vigorous fountains extended from just northeast of Alae to within 600 m of the base of Kane Nui o Hamo. The eastward extension took place in a series of en echelon segments successively offset to the south (fig. 1). Fountains reached heights of about 40 m near the east end of the line, building up a large spatter cone (vent C). Fissures continued to open toward Kane Nui o Hamo,



begun in April 1969 at the site indicated; this program was ended on May 24 when new lava flooded the crater, overwhelming the drilling equipment.

reaching the base by 1045; shortly thereafter fountaining began from fuming new cracks on the northwest flank of the hill (vent D).

Two pahoehoe flows poured rapidly southward from the fissures, crossing the Chain of Craters Road at about 1030. A small part of the easternmost flow, fed chiefly by vent C, flooded the tourist overlook at Makaopuhi Crater, spilled over the rim, and plummeted 230 m to the floor (figs. 9 and 10), where it spread slowly outward in craggy lobes of aa. The flow advanced with such force that it swept heavy equipment into the crater, including parts of a water trailer parked near the rim and a heavy A-frame anchoring a tramway used in drilling operations within the crater. Eventually 90 percent of the surface of the March 1965 lava lake (Wright and others, 1968) was covered by an aa flow about 3 m thick. Outside of Makaopuhi, the main part of the flow continued advancing downslope, following the Chain of Craters Road until it stopped about 2.3 km south of Makaopuhi (fig. 11). The lava flowed as fluid pahoehoe from the vent to Makaopuhi, then, with cooling, degassing, and crystallization, became less fluid and gradually changed over a distance of 200–300 m into aa, which extended to the end of the flow.

The second of the two flows, fed largely by vent A,

crossed the Chain of Craters Road midway between Alae and Makaopuhi Craters (pl. 1; fig. 1). This flow also

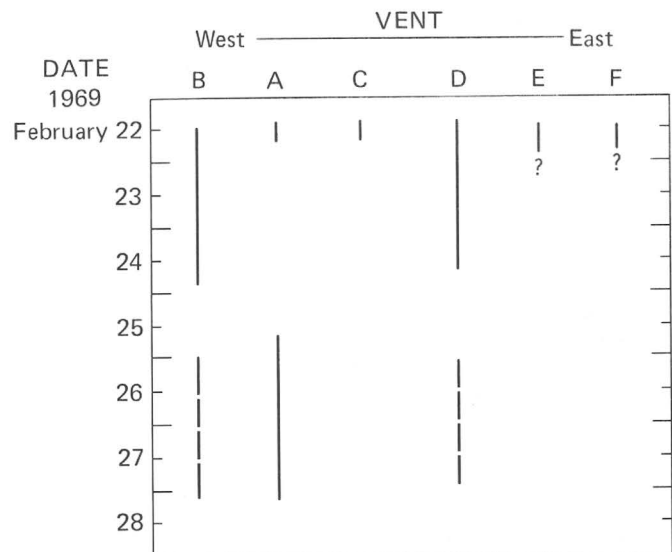


FIGURE 8.—Time and duration of eruptive activity at selected vent areas near and east of Alae Crater during the February 1969 eruption. See figure 1 for location of vent areas. Dashed line, vent sporadically active. Query, time uncertain.



FIGURE 9.—Aerial view of Makaopuhi Crater, showing dark aa flow erupted on February 22, 1969, covering 90 percent of floor of deep pit. The aa was fed by 230-m-high cascades, as part of light-hued pahoehoe flow (lower right) spilled over crater rim. The rest of the pahoehoe flow advanced down the Chain of Craters Road (background), changing to aa. Note fallen trees along broad edge of flow in lower right. Prominent dark aa flow, center right, also erupted on February 22. Arrow indicates location of tourist overlook. Photograph taken in March 1969.

changed to aa downslope and eventually joined the first flow a short distance south of Makaopuhi. A National Park Ranger returning from having conducted tourists out of the area was trapped in his car between the two flows, spending a perilous 8 hours amid falling pumice, choking fume, and smoke from the burning forest before a daring helicopter rescue. Only natural levees built by the westernmost flow and an old spatter rampart south of vent C that diverted the lava prevented the Ranger and his car being inundated. His car remained as a landmark until flooded by lava in 1972.

The fissure system had been slowly lengthening westward from vent A. By 1130, it had reached the rim of Alae Crater, and by 1200 a segment of the erupting fissure was slowly splitting the mezzanine and western crater wall (vent B). Spectacular 50-m-high cascades poured from the roaring fountains into the inner pit of the crater, feeding a rapidly deepening pool of molten lava. Details of the formation of this lava lake are given by Swanson, Duffield, Jackson, and Peterson (1972).

The fissure reached the west rim of Alae Crater at 1227 and continued its slow westward migration, accompanied by fountains a few metres high. Some of the lava from these fountains flowed into Alae, joining lava

being erupted within the crater to form an impressive two-tier cascade (fig. 12). By 1245, hairline cracks had started to form across the Chain of Craters Road along strike of the fissure, and observers on the south rim of Alae were evacuated to safe points west of the cracks.

The opening of the fissure across the Chain of Craters Road west of Alae Crater and the beginning of fountaining from it were observed and measured (fig. 13). A crack cutting the asphalt pavement, barely visible at 1323, was 5 minutes later about 1.5 cm wide and opening at a rate of 4 mm/min (fig. 13A). The rate of opening abruptly increased to 5 mm/min at 1343, when fountains were within 100 m of the road. Displacement along the crack was predominantly perpendicular to the strike but there was some vertical displacement, with the north side up 3 cm. The asphalt pavement buckled almost randomly as it adjusted to the underlying ground cracking. By 1350 (fig. 13B) 20-m-high fountains played from the fissure only 65 m away, and at 1355 the crack, which by then was 12 cm wide, began closing at a rate of 3 mm/min. We abandoned the site at 1357, when the crack began to steam and fume heavily (fig. 13C), withdrew about 20 m, and watched gassy lava surge from it 2 minutes later. Fountaining was sluggish for the first 2 minutes (fig. 13D), apparently as energy was expended in widening the fissure to its eventual width of nearly 1 m, but soon became quite vigorous (fig.

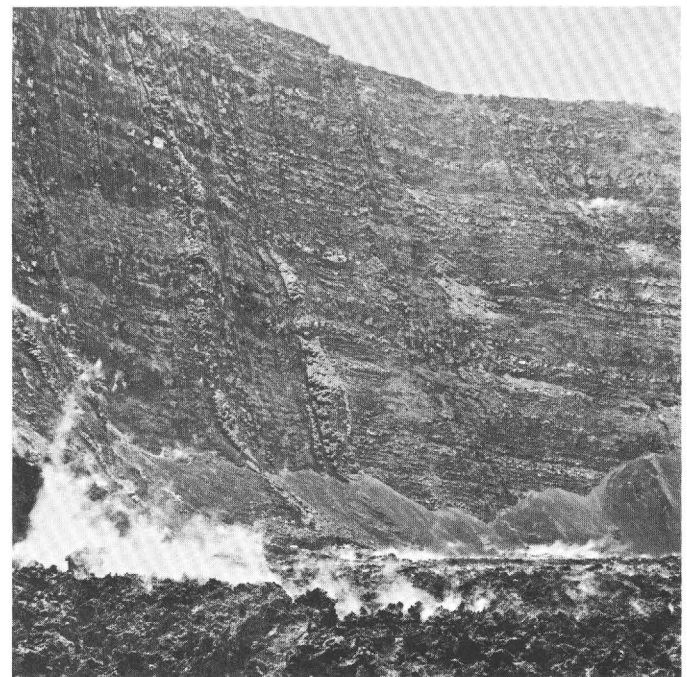


FIGURE 10.—Lava drapery on 230-m-high walls of Makaopuhi Crater. View from floor of deep pit, March 5, 1969. Note talus cones at base of crater wall, built predominantly from falling aa fragments, with minor amounts of dislodged wallrock included. Steam rises from cooling aa on floor of crater.

13E). Gradually the fountaining extended westward along the still advancing fissure; by 1420 fountaining had nearly died out at the road but was strong about 25 m farther west.

By 1545, the fissure had split open to a point 500 m due south of Alo'i Crater, its maximum westerly extent, and low fountains played from several vents near its end. Lava erupted from this fissure merged into a thin pahoehoe flow that advanced southeastward, burning dense jungle and creating many tree molds.

In late afternoon, fountaining was still vigorous at vent B in Alae Crater but had stopped at vents A and C (fig. 8). Most of the area between Alae and Kane Nui o Hamo was covered by new flows. A line of fountains 150–200 m long was centered over vent D; the fountains, more than 100 m high, fed a flow that covered much of the flat at the base of Kane Nui o Hamo and extended 3 km eastward. En echelon segments of the fissure were active on the north and northeast flanks of Kane Nui o Hamo; the easternmost vent (E) sent a tongue of slabby pahoehoe across the trail to Napau Crater and small lobes of aa into Napau (fig. 14). Fume was rising farther downrift; flights in a Civil Air Patrol plane later showed that small flows had issued quietly from three locations as far as 7 km northeast of Kane Nui o Hamo; the easternmost of these vents is designated vent F. These vents lie along fissures that trend somewhat more easterly than those associated with vents A–E. Fur-



FIGURE 11.—Aerial view of aa flow that followed Chain of Craters Road southward from Makaopuhi Crater (right background). Road gradient, 4.6 m/km; flow, 2–3 m thick. The Kalapana Trail (left edge) parallels road.

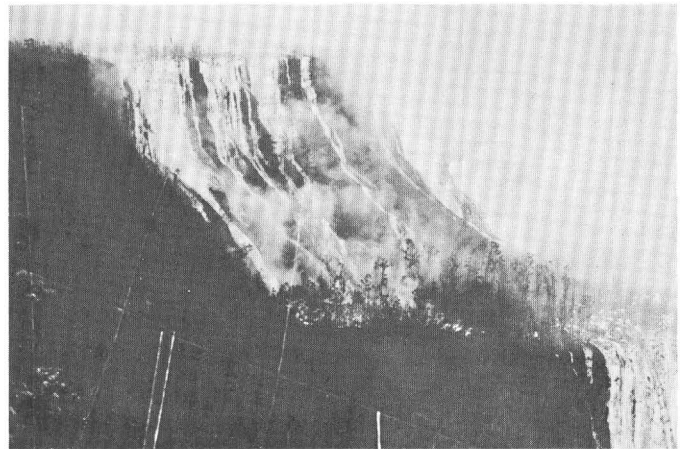


FIGURE 12.—Two-tier lava cascade into Alae Crater. View from south rim, midday February 22, 1969. Lava (left) cascading 80 m into crater and lava from spurting fountains (visible near right edge) join and pool on mezzanine before plunging 50 m into inner pit (lower right corner).

thermore, the fissures are considerably north of the projected fissures near Kane Nui o Hamo, when the right-offset en echelon pattern is taken into account.

Fountaining along the entire length of the fissure system west of Alae Crater resumed that evening but died out during the early morning. By daybreak on February 23, a row of spatter cones as high as 10 m extended westward almost a kilometre from the crater rim (fig. 15). Vigorous fountaining continued at vent B in Alae; by afternoon, a lava lake more than 50 m deep filled the inner pit of the crater (fig. 7; Swanson and others, 1972). Vent B continued to erupt until about 1715 February 24, 2 hours after fountains from vent D had died (fig. 8).

No activity was observed for almost a day; then at 1500 February 25, vent A reopened and fountaining began. Fountains as high as 65 m fed a pahoehoe river that flowed westward and cascaded into Alae. A large pool of lava, ponded behind its own natural levees south and east of vent A, persisted until the end of the eruption. Occasionally the pool spilled over its levees and fed lava down the westernmost of two flows that had trapped the National Park Ranger.

Small vents near the base of Kane Nui o Hamo and within Alae Crater reopened for periods of a few hours between February 25 and 28. All activity had ended by about 0300 February 28, although foundering of the solid crust on the Alae lava lake, similar to that described and interpreted by Shaw, Kistler, and Evernden (1971, p. 878) in the 1965 Makaopuhi lava lake, continued until the night of March 1–2, and liquid lava oozed to the surface of the lake from one small rootless vent on March 5 (fig. 7).

When the eruption ended, a lava lake 70 m deep

containing  $7 \times 10^6 \text{ m}^3$  of lava partly filled Alae Crater (fig. 7; Swanson and others, 1972, fig. 4B) and large new spatter cones as high as 35 m had been built over vents A, C, and D. The Chain of Craters Road had been cut by lava flows for the first time in history. An area about  $6 \text{ km}^2$  was covered by new pahoehoe and aa flows; estimates of thickness indicate that these flows had a volume of about  $13 \times 10^6 \text{ m}^3$ . The total volume of erupted lava, uncorrected for vesicularity, is about  $20 \times 10^6 \text{ m}^3$ ;

this figure may be in error by as much as 25 percent, primarily because of difficulties in estimating the thickness of the flows.

#### PETROGRAPHY AND CHEMISTRY OF THE LAVA

The February 1969 lava is olivine-poor tholeiite that contained less than 6 percent crystals upon eruption (tables 2 and 3). The phenocryst minerals are olivine plus included spinel, clinopyroxene, and normally zoned

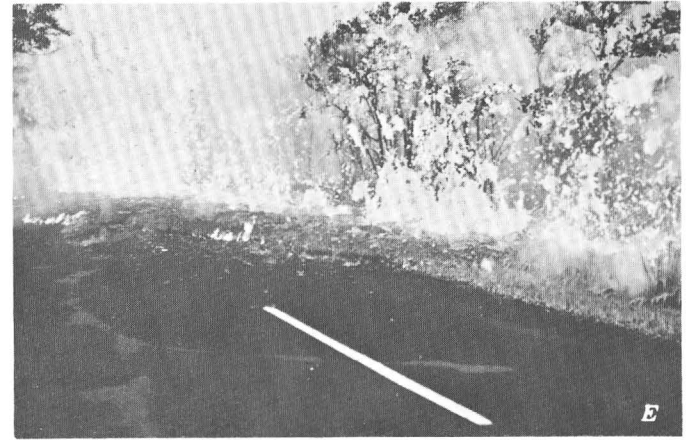


FIGURE 13.—Opening of and initiation of fountaining from a fissure across Chain of Craters Road west of Alae Crater, February 22, 1969. *A*, 1328. As nearly straight fissure opens beneath it, the asphalt pavement responds irregularly. *B*, 1350. Uppermost layer of asphalt has buckled and slid across underlying layer. Ground crack beneath asphalt pavement (not shown) about 10 cm wide. *C*, 1358. Steam and fume issuing from fissure. Spatter falls on road surface from fountains near left edge of pavement. *D*, 1401. Lava surging from fissure uplifts pavement and wells out as sluggish flow. Note spatter clots flying through air; steam issuing from extension of crack on right side of road. *E*, 1408. Lava fountains from fissure extending into forest on right side of road, setting fires and forming tree molds. Lava flow advances along highway, causing asphalt to melt and, in places, burn. Asphalt pavement buried by thin flow can commonly be located and mapped by observing black discoloration of flow by tarry substances distilled from the asphalt. Photograph *E* by J. C. Forbes.



FIGURE 14.—Small lobes of newly erupted aa pool at the base of 40-m-high northwest wall of Napau Crater. Lava was erupted from vent E on northeast slope of Kane Nui o Hamo, about 2 km from upper left corner of view. Floor of crater is crusted lava erupted in October 1968; steam issues from one of October fissures.

labradorite in order of appearance and abundance. Most phenocrysts are small, generally less than 1 mm in diameter, but some single crystals and glomeroporphyritic clots of olivine are more than 2 mm in diameter.

The range in composition of the six chemically analyzed samples is small and by itself shows no obvious relation to time or location of eruption (table 2). Modal analyses suggest that on February 22 vent C erupted more olivine-rich lava (average of 4.7 percent, table 3) than the other vents (average of 1.3 percent), and the chemically analyzed sample from vent C has more MgO than the other analyzed samples.

Temperatures were not measured during the eruption because the vents could not be approached closely,

TABLE 2.—Chemical analyses of lava from the February 1969 eruption of Kilauea Volcano

[Analyzed by V. C. Smith using methods described by Peck (1964)]

Field No.	A169-1	A169-6	A169-7	A169-12	A169-13	A169-15
SiO <sub>2</sub>	50.24	50.50	50.27	50.18	50.17	49.97
Al <sub>2</sub> O <sub>3</sub>	13.44	13.53	13.38	13.28	13.25	13.11
Fe <sub>2</sub> O <sub>3</sub>	1.41	1.79	1.35	1.25	1.70	1.83
FeO	9.90	9.50	9.99	10.08	9.72	9.60
MgO	8.05	7.56	8.06	8.58	8.48	9.06
CaO	10.96	11.08	11.00	10.85	10.83	10.58
Na <sub>2</sub> O	2.31	2.31	2.27	2.26	2.28	2.24
K <sub>2</sub> O	.48	.50	.49	.47	.48	.47
H <sub>2</sub> O <sup>+</sup>	.07	.00	.05	.00	.16	.11
H <sub>2</sub> O <sup>-</sup>	.00	.03	.00	.01	.01	.01
TiO <sub>2</sub>	2.59	2.67	2.62	2.54	2.56	2.57
P <sub>2</sub> O <sub>5</sub>	.26	.27	.25	.26	.26	.26
MnO	.17	.18	.17	.18	.17	.17
CO <sub>2</sub>	.02	.02	.02	.02	.02	.02
Cl	.01	.01	.01	.01	.01	.01
F	.04	.04	.04	.04	.04	.04
Subtotal	99.95	99.99	99.97	100.01	100.14	100.05
Less O	.02	.02	.02	.02	.02	.02
Total	99.93	99.97	99.95	99.99	100.12	100.03

A169-1. Pumice erupted from vent A between 1000 and 1130, February 22. Collected at time of eruption along road between Alae and Makaopuhi Craters.  
 A169-6. Glassy flow crust erupted from vent F, probably on February 22. Collected on March 19.  
 A169-7. Spatter erupted from vent D, probably on February 24. Collected on July 23.  
 A169-12. Spatter erupted from vent A, probably February 26 or 27. Collected on July 28.  
 A169-13. Glassy crust on flow erupted from vent E on February 22. Collected on July 31 where flow crossed the trail between Makaopuhi and Napau Craters.  
 A169-15. Aa from floor of Makaopuhi Crater, erupted from vent C on February 22. Collected on August 3.

but maximum temperatures can be estimated from the iron:magnesium ratios of the analyzed samples by using the melting curve for Kilauea lavas (Thompson and Tilley, 1969, fig. 1). These temperatures (table 4), adjusted for phenocryst content, show only a 20°C range, 1185° to 1205°C. The coolest lava (highest iron:magnesium ratio) comes from the easternmost vent (F); this is consistent with the interpretation that cooling occurred during shallow transport within the rift system. The estimated temperatures are probably too high, because Thompson and Tilley's melting runs were conducted under anhydrous conditions, whereas during eruption the actual lava contained water and other volatiles. Judged by the presence of small amounts of pyroxene and plagioclase phenocrysts in some samples, actual eruption temperatures were probably in the range 1160–1180°C (Wright and Weiblen, 1968; Thompson and Tilley, 1969, fig. 1).

Wright, Swanson, and Duffield (1975) examined the chemistry of the February 1969 lava within the context of other 1968–71 east rift eruptions. They found that the

TABLE 3.—Modal analyses in volume percent of lava from the February 1969 eruption of Kilauea Volcano  
 [Plus or minus values indicate differences between mean and each of two counts of 500 points. Tr., trace]

	A169-1	A169-4	A169-5	A169-6	A169-7	A169-9	A169-11	A169-12	A169-13	A169-14	A169-15	A169-16
Glass + quench	99.4	99.6±0	97.8±1.2	97.6±0.8	98.0±0	98.2±0.6	94.1±0.3	97.9±0.3	97.6±0.4	94.8±3.6	96.6±1.6	98.9±0.1
Phenocrysts												
Olivine + spinel	.6	.4±0	2.1±1.3	1.9±0.9	1.6±0	6±0	5.5±0.3	2.0±0.4	1.9±0.5	5.2±3.6	3.4±1.6	1.0±0
Clinopyroxene			.1±0.1	.3±0.1	.4±0	1.0±0.6	.3±0.1	.1±0.1	.3±0.1			.1±0.1
Plagioclase				.2±0		.2±0	.1±0.1	Tr.	.2±0			Tr.
Number of points	721	1000	1000	1000	1000	1000	1000	1000	1000	1000	1000	1000
Vent	A	B	A	F	D	D-E	C	A	E	C	C	F

<sup>1</sup>Includes abundant small microlites of pyroxene and plagioclase.

A169-1  
 A169-6  
 A169-7  
 A169-12  
 A169-13  
 A169-15 } Chemically analyzed samples; see table 2.

A169-4. Spatter erupted from vent B on February 22.  
 A169-5. Crust of pahoehoe flow from vent A, collected while flowing on February 28.  
 A169-9. Spatter erupted from short fissure between vents D and E on February 22.  
 A169-11. Spatter erupted from vent C on February 22.  
 A169-14. Crust of pahoehoe flow erupted from vent C on February 22 and collected at rim of Makaopuhi Crater.  
 A169-16. Crust on block from aa flow erupted from western end of vent F on February 22.



FIGURE 15.—Aerial view showing row of spatter cones formed during the night of February 22–23, 1969, extending westward from the west rim of Alae Crater. Chain of Craters Road is buried by new lava, almost all of which flowed toward the south (right), the prevailing slope direction. Photo by Don Reeser, National Park Service.

February lavas are hybrid, having compositions that can be explained by mixing magma of 1967–68 summit vintage with that erupted later during the summer and

TABLE 4.—*Estimated maximum eruption temperatures of February 1969 lava, Kilauea Volcano*  
[Temperature from Thompson and Tilley (1969, fig. 1)]

Field No.	Vent	$\frac{\text{FeO} + \text{Fe}_2\text{O}_3}{\text{MgO} + \text{FeO} + \text{Fe}_2\text{O}_3}$		Temperature °C
		Bulk	Glass adjusted for phenocrysts <sup>1</sup>	
A169-1	A	0.584	0.587	1195
A169-12	A	.569	.577	1205
A169-15	C	.558	.571	1205
A169-7	D	.585	.592	1195
A169-13	E	.574	.583	1200
A169-6	F	.599	.609	1185

<sup>1</sup>Using modes (table 3) and  $\frac{\text{FeO} + \text{Fe}_2\text{O}_3}{\text{MgO} + \text{FeO} + \text{Fe}_2\text{O}_3}$  ratios of 0.200 (olivine), 0.352 (clinopyroxene), and 0 (plagioclase).

fall of 1969 and with lesser amounts of differentiated magma like that erupted in October 1968 (Jackson and others, 1975). In general, the February lava is more nearly like the early lava erupted during the 1969–71 Mauna Ulu eruption than that of the two preceding 1968 rift eruptions (Wright and others, 1975; Swanson and others, 1971).

#### SEISMIC ACTIVITY DURING THE ERUPTION

Heightened seismic activity within the upper east rift zone that began at about 0630, February 22, was the first warning of impending eruption (fig. 16B, C). The Makaopuhi (MPH) seismograph began recording small, shallow (focal depths less than 5 km) earthquakes at a rate of about 1 per min in a background of weak, sporadic harmonic tremor. The tremor gradually increased in amplitude, became continuous by 0900, and

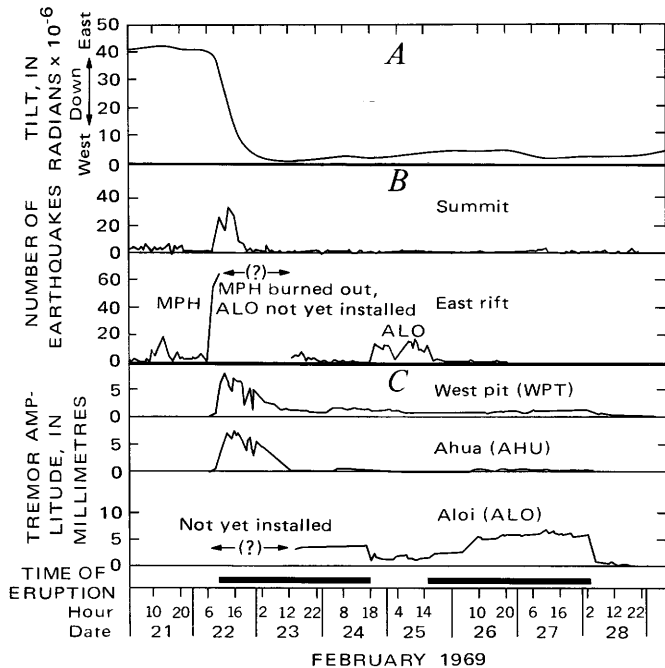


FIGURE 16.—Summary of tilt and seismicity during the February 1969 eruption. *A*, Ground tilt. Record from continuously recording, mercury-pool tiltmeter at Uwekahuna that gives only east-west component of tilt. *B*, Earthquake counts. Summit earthquakes recorded on North Pit (NPT) smoked seismographs; east rift earthquakes recorded by Makaopuhi (MPH) and Aloi (ALO) seismographs. All earthquakes with peak-to-peak amplitude less than 5 mm obscured by harmonic tremor in both summit and east-rift areas. *C*, Tremor amplitude from three seismograph stations. Relative amplitude indicates qualitatively the "vigor" of tremor. Earthquakes and tremor amplitudes from east rift for part of February 22–23 not plotted, as key stations, Makaopuhi and Aloi, were out of operation. See figure 1 for locations.

increased sharply again at 0950 when fountaining began at vent A. Shortly thereafter, lava flows burned out the cable transmitting signals to the observatory from MPH. As a result, we do not adequately know the seismic pattern on the rift during the first day of the eruption; the Aloi (ALO) seismometer was not installed until the following day and most of the rift earthquakes were too small to be recorded by more distant seismographs. Presumably the number of earthquakes in the eruption area dropped substantially during the afternoon of February 22 after all new vents had opened. Numerous quakes with magnitudes of about 1 to 2 were recorded on February 22–23 from the general area of the eruption, using additional stations in the seismic network.

At the summit, the hourly number of shallow caldera earthquakes first decreased when deflation began, then increased as the rate of deflation picked up (fig. 16*A, B*). These earthquakes, most of which were small ( $M \leq 2.6$ ) and shallow (focal depth 5 km or less), continued throughout the period of deflation and were most frequent when the rate of deflation was at a maximum. As

deflation ended and slow reinflation began, caldera earthquakes became less frequent.

Tremor in the summit area was at maximum strength from the start of the eruption until the early morning of February 23. Sharp drops in tremor amplitude at about 1905–1958 and 2150–2248 February 22 reflect the fluctuating nature of the tremor (fig. 16*C*). Early on February 23, the tremor amplitude decreased and remained nearly constant until the end of the eruption.

The Aloi seismometer, installed at midday February 23, immediately began recording constant tremor and a few small earthquakes (fig. 16*C*). Harmonic tremor near the rift zone subsided markedly at 1715 February 24, when the eruption temporarily stopped, then increased on February 25, when fountaining resumed. Tremor became stronger at about 0500 February 26, coincident with resumption of vigorous fountaining, continued at roughly constant strength until 0255 February 28, then declined rapidly as the eruption ended. Traces of weak tremor were recorded for more than 14 hours after the end of the eruption.

Earthquakes during and immediately preceding the eruption took place primarily in two areas (fig. 17), Kilauea Caldera and the vicinity of the eruption itself. This pattern is typical of east rift eruptions. The earthquake activity in the caldera is associated with the area

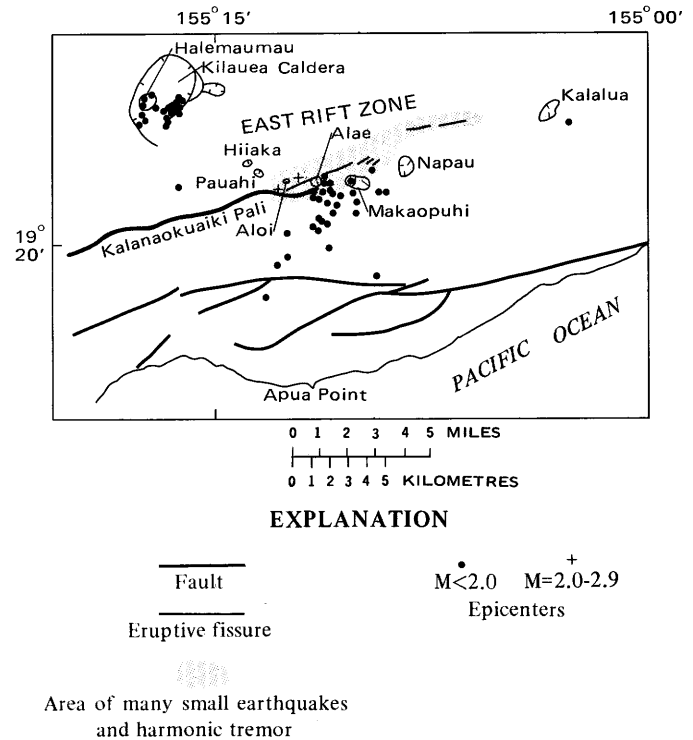


FIGURE 17.—Epicenters and magnitudes of earthquakes with focal depth less than 10 km from 0523 February 22 to February 28, 1969. Epicenters are shown for earthquakes that were adequately recorded and located.

of maximum subsidence and contraction (figs. 20 and 21); deformation and seismicity are presumably related to withdrawal of magma from the shallow reservoir complex. The earthquake activity near the eruption site apparently results from the forceful intrusion of magma from conduits within the rift zone toward the surface.

The epicentral area on the rift zone extends southward from the eruption site, and most of the larger, well-recorded earthquakes occurred south of the rift. As the eruption continued, the area of earthquake activity enlarged still farther southward. Koyanagi, Swanson, and Endo (1972) found this pattern of events to be common during east rift eruptions and related it to southward displacement of the south flank as a result of diking in the rift zone.

Near and shortly after the end of the eruption, several relatively large (largest of  $M=3.6$ ), 15- to 35-km-deep earthquakes occurred beneath the summit region and within the south flank in an area 5–10 km southwest of the caldera (fig. 2D). Short bursts of harmonic tremor, probably deep judged by a comparison of relative tremor amplitudes throughout the network, were also recorded during this period. These events may be related to the replenishment of magma in the partly evacuated shallow reservoir system beneath the caldera.

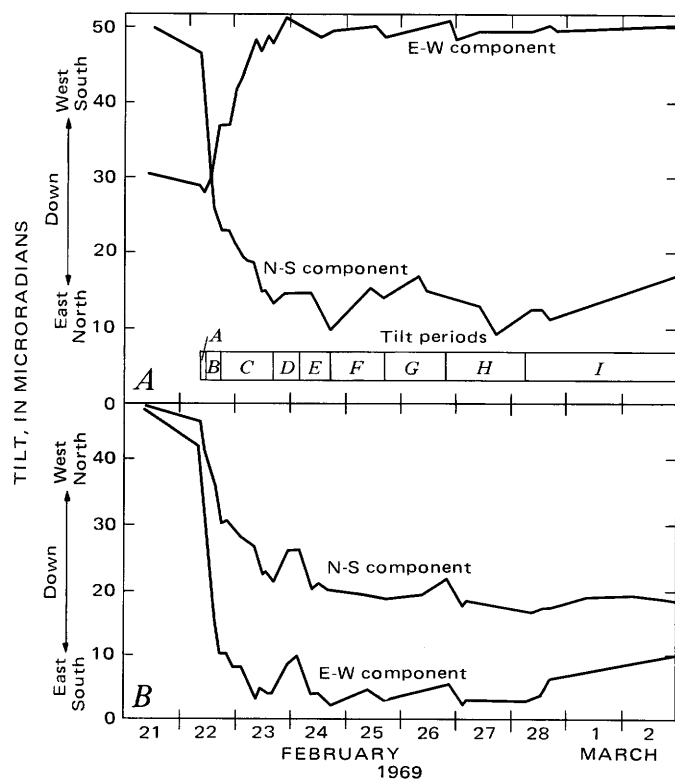


FIGURE 18.—Tilt records between 0700 February 21, and 2400 March 2, 1969. Daily readings are from short-base water-tube tiltmeters. The tilt periods indicated represent intervals keyed to figure 19. A, Outlet (OTL) vault. B, Uwekahuna (UWE<sub>sb</sub>) vault. Location of the tiltmeters shown in figure 1.

Weak long-period earthquakes were recorded at the summit during the brief reinflation period from February 23 to 26. Such long-period quakes are commonly associated with periods of inflation during flank eruptions (Koyanagi and Endo, 1971, p. C164) and perhaps result from structural readjustments to movement of magma into the reservoir system.

The onset of seismic activity immediately before the February 1969 eruption was less sharply defined than before the August and October 1968 eruptions (Jackson and others, 1975), and the overall seismicity was not as strong. Yet the volume of February lava was far greater. Perhaps the intense ground fracturing during the 1968 activity opened new conduits or widened old ones within the rift zone, permitting voluminous intrusion of magma with comparatively little rupturing.

#### GROUND DEFORMATION IN THE SUMMIT AREA

Moderate ground deformation, consisting of inward tilting, subsidence, and horizontal contraction, occurred in the summit area during the eruption. All three modes of deformation are in general agreement as to the site of maximum deflation, but each gives additional information concerning the timing or nature of the event. The deformation in most ways typifies that accompanying Kilauea flank eruptions and is related to the withdrawal of magma from the shallow storage system beneath the caldera.

#### TILT

Strong summit deflation began at 0800 February 22 (fig. 16A and 18), as magma began to leave the summit storage system. By 0950, when the eruption began, deflationary tilt amounted to  $5 \mu\text{rad}$  per hour. The rapid summit deflation coincided with a sharp increase in the frequency of shallow summit earthquakes (fig. 16A, B). By 1800 February 22, both the rate of summit deflation and the frequency of summit quakes had decreased, suggesting that the rate of eruption nearly equaled the rate of recharge of the summit reservoir from a deeper source. By 0700 February 23, the major summit deflation had ended, although the eruption still continued, and the recording tiltmeter in Uwekahuna vault began registering a slight inflationary tilt. This inflation continued until 1800 February 26 (fig. 16A), when slow deflation resumed and continued until the eruption ended, at which time inflation began once again.

Between 1600 February 23 and about 1700 February 24, a small inflation-deflation cycle is conspicuous on both components of the Uwekahuna short-base water-tube tiltmeter and on the north-south component of the Outlet short-base water-tube tiltmeter (fig. 18A, B) but did not register on the recording tiltmeter (fig. 16A). We have no explanation for the failure of the recording tiltmeter to track this event, which we feel must be real

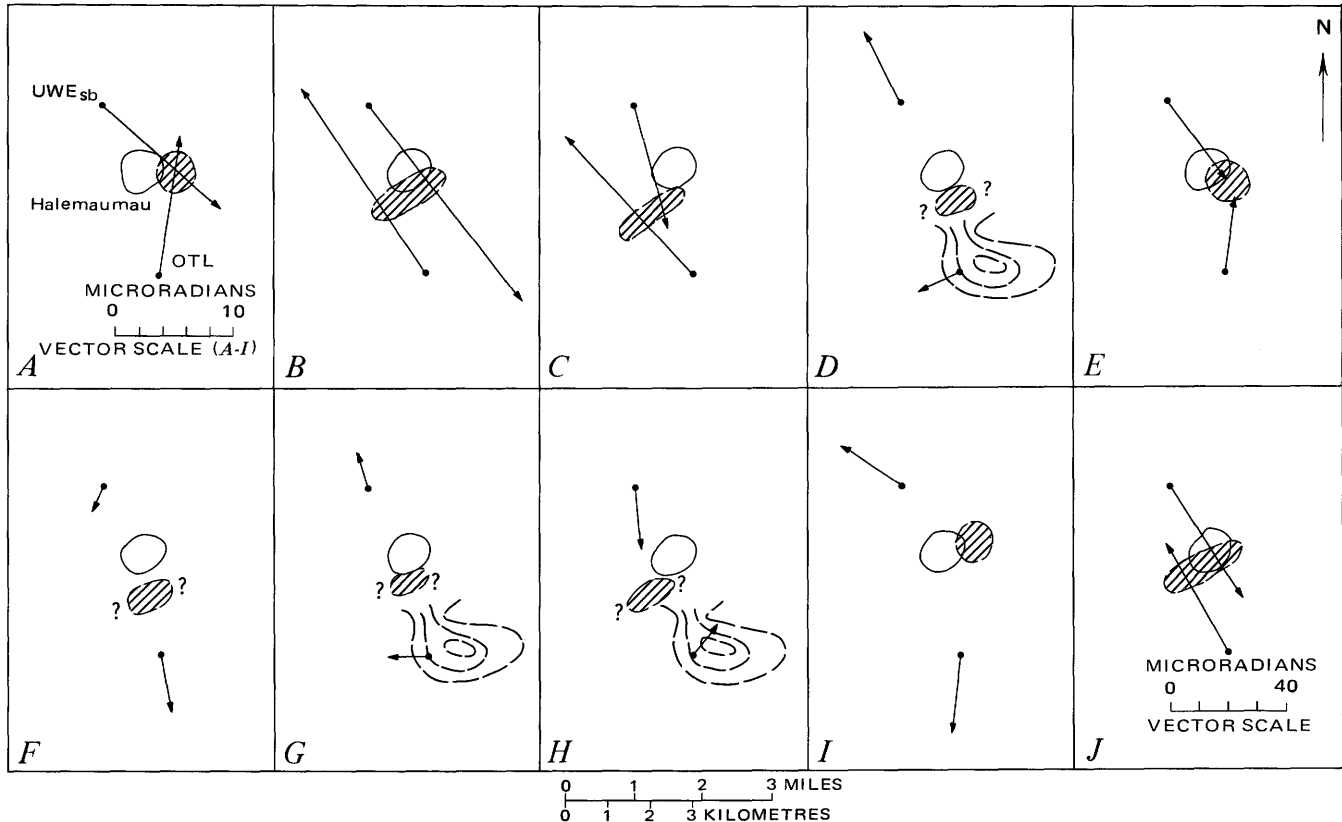


FIGURE 19.—Ground tilt changes (vectors) for short-base water-tube tiltmeters at Uwekahuna (UWE<sub>sb</sub>) and Outlet (OTL) vaults for 10 periods between 0700 February 22 and 2400 March 2, 1969. *A*, 0700 to 1100 February 22. Deflation begins. *B*, 1100 to 1700 February 22. Deflation. *C*, 1700 February 22 to 1600 February 23. Deflation. *D*, 1600 February 23 to 0400 February 24. Slight inflation. *E*, 0400 to 1700 February 24. Deflation. *F*, 1700 February 24 to 1700 February 25. Fountains stop. *G*, 1700 February 25 to 2000 February 26. Fountains start. *H*, 2000 February 26 to 0600 February 28. Defla-

tion. *I*, 0600 February 28 to 2400 March 1. Eruption ends. *J*, Summation of *A* to *H*. Note vector scale smaller than in *A*–*I*. Diagonals show probable location of deformation centers as defined by tilt vectors; query indicates uncertain location. Dashed contours, *D*, *G*, and *H*, indicate subsidiary area of horizontal contraction, as shown in figure 21. Vectors from the Uwekahuna tiltmeter have been rotated 20° clockwise, an empirical adjustment found necessary during periods of rapid summit deflation.

despite the comparative imprecision of the water-tube meters.

The changing location of the deformation centers as the eruption progressed can be documented in an approximate manner, as the short-base water-tube tiltmeters at Uwekahuna and Outlet were read several times daily between 0700 February 22 (3 hours before the eruption) and 2400 March 2. Summit deflation was initially centered near the east side of Halemaumau but migrated 1 km or more to the southwest by 1600 February 23, as shown by figure 19*A*–*C*. Slight inflation then occurred over the next 12 hours (fig. 19*D*), probably centered in two areas—near the site shown in figure 19*C* and near the site of the dilatation minimum (fig. 21) slightly east of Outlet vault—for the Uwekahuna vector appears too large to be reflecting the same source as the Outlet vector. Deflation centered near Halemaumau began again in the early morning of February 24 (fig. 19*E*). Late in the afternoon, all fountaining ceased and the summit immediately responded with inflation cen-

tered north of Outlet vault (fig. 19*F*), although the Uwekahuna vector had not yet completely rotated to the northwest at the time the tilt was read at 1700 February 25. Fountaining resumed at 1500 February 25, but inflation centered north and east of Outlet continued until about 2000 February 26 (fig. 19*G*); apparently the rate of magma recharge was greater than the rate of eruption. Summit deflation began again at about 2000 February 26 and continued until the eruption ended in the early morning of February 28 (fig. 19*H*); this deflation, like the brief inflation on February 23–24 (fig. 19*D*), was centered at two locations north and east of Outlet. Immediately after the eruption stopped, inflation began at nearly the exact location of the initial deflation center (fig. 19*A* and *I*).

The detailed tracing of the migration of deformation centers demonstrates again the complexity of the reservoir system. Nonetheless, one generality is apparent for periods of inflation and deflation: the deformation is initially centered east or northeast of Halemaumau and

migrates southward with time. This pattern, found true for previous eruptions (Fiske and Kinoshita, 1969; Jackson and others, 1975), holds for both the inflation before and the deflation during the February 1969 eruption (figs. 3 and 19).

The summation of tilt over the entire eruption (fig. 19J) shows that the net deflation center was located near the south side of Halemaumau and was possibly elongate in a northeast-southwest direction. This center is very close to that defined by the subsidence contours (fig. 20), particularly considering that the leveling interval spans part of the preeruption and posteruption periods of inflation.

**VERTICAL DISPLACEMENT**

The summit area of Kilauea subsided markedly dur-

ing the eruption (fig. 20). A center of subsidence elongate in a north-south direction, with a maximum displacement of 11.5 cm at a bench mark 0.5 km northeast of Halemaumau, is defined by contours of equal displacement relative to an arbitrary datum point about 8 km away. This center is consistent with that defined by the long-base water-tube tilt data for the same period (fig. 20), after the azimuth of the Uwekahuna tilt is adjusted as described previously. Presumably the subsidence took place during periods of inward tilting, the most rapid displacement accompanying the most rapid tilting. If it did, then the maximum rate of subsidence may have been about 1 cm/hr.

The volume of net subsidence over the survey interval is about  $3.7 \times 10^6 \text{ m}^3$ , assuming that the outer fringe of the subsidence bowl is roughly concentric about the

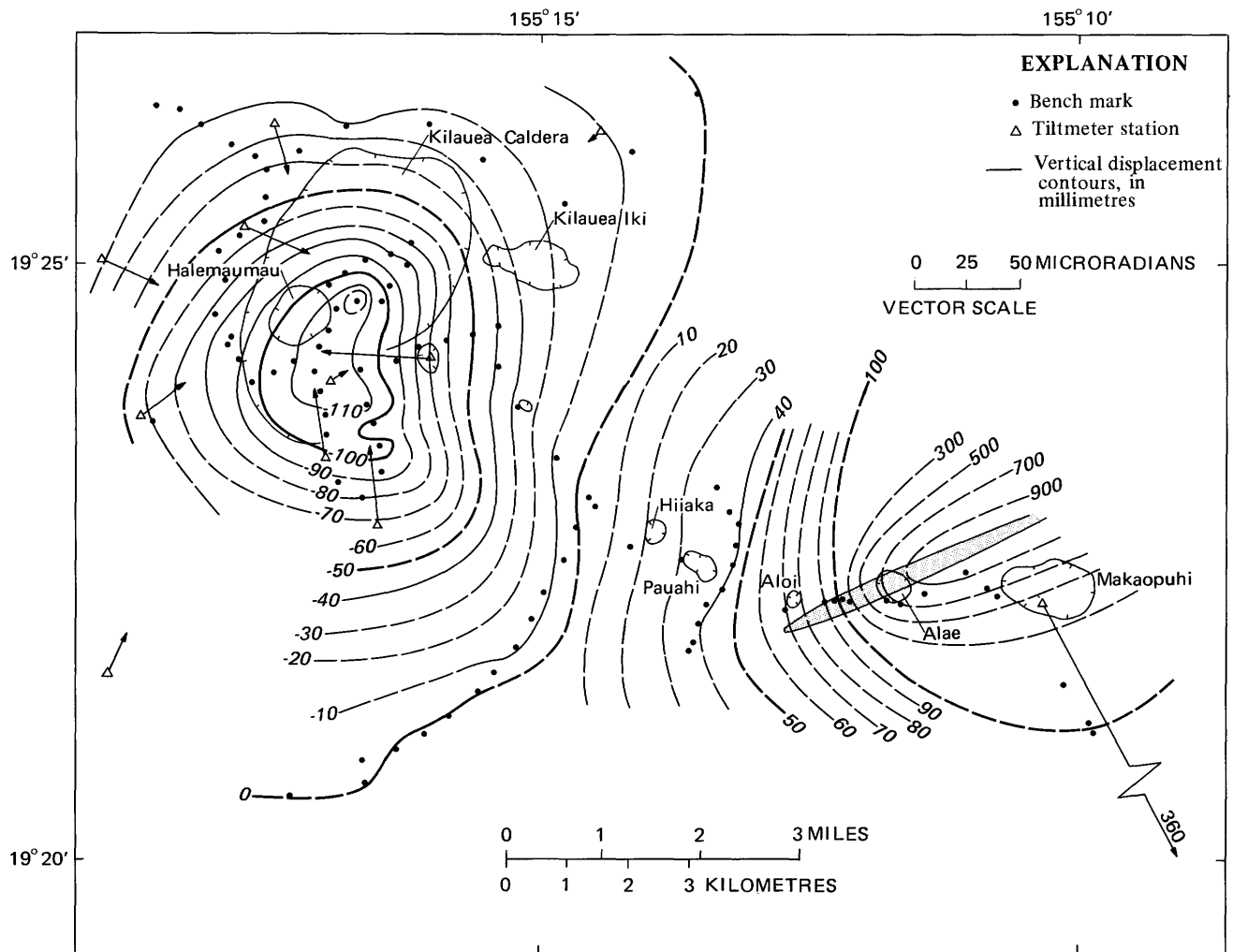


FIGURE 20.—Ground tilt (vectors) and vertical displacement (contours) between February 4–5 and March 3–5, 1969, showing deformation resulting largely from February eruption. Arbitrary leveling datum point is northernmost bench mark. Shaded area along zone of eruptive fissures, approximate location of a keystone graben not depicted by contours; see text for discussion. Tilt at station southeast of eruption area,  $360 \mu\text{rad}$ . Contour interval 200 mm in eruption area, 10 mm elsewhere. The  $-115 \text{ mm}$  contour in the summit area more precisely defines location of maximum subsidence. Dashed contours, uncertain location.

center. This figure is a minimum volume for the eruption itself, because (1) small but significant episodes of uplift immediately preceded and followed the eruption between the times of the two surveys and (2) it is possible that the datum point subsided slightly.

The February subsidence was only moderate compared with that accompanying many other flank eruptions, despite the unusually large volume of erupted lava. For example, the maximum displacement was 19 cm during the August 1968 eruption and 25–30 cm during the March 1965 eruption (Jackson and others, 1975; Wright and others, 1968).

The location of the center of subsidence was different for the February eruption than for eruptions involving larger subsidence. After migrating southward, most large subsidence events at Kilauea eventually become centered about 1.5–2 km southeast of Halemaumau (Jackson and others, 1975), whereas the February subsidence was centered about 2 km farther north, according to the combined tilt and leveling information (figs. 19J and 20). The combination of the smaller volume and more northerly center of subsidence suggests that the reservoir complex beneath the caldera failed to empty as completely as it had during previous eruptions. The February data show a small, shallow basin open to the west in the south part of the caldera subsidiary to the major center (fig. 20). This basin, which coincides in location with a local area of contraction (fig. 21), lies close to the usual overall deformation center and may reflect an arrested stage in the final emptying of the reservoir.

#### HORIZONTAL DEFORMATION

The summit area of Kilauea contracted horizontally as well as subsided during the eruption (fig. 21). Ground displacements were computed from geodimeter measurements assuming a stable base line (as indicated in the caption to fig. 5). The maximum measured displacement, at HVO-118, was more than 10 cm. The overall pattern of displacement shows a major center of contraction located near the east rim of Halemaumau Crater, and contours of negative dilatation define a similar center with an amplitude of more than  $-8 \times 10^{-5}$ . This dilatation center is remarkably close to that defined by the other deformation data (fig. 20), considering that the two-dimensional strain values were arbitrarily plotted at the center of gravity of each strain polygon.

The dilatation contours indicate a secondary center of contraction in the southern part of Kilauea Caldera (fig. 21). Displacement vectors do not show this center clearly, although the magnitudes and azimuths of displacements at HVO-119 and HVO-132 may partly reflect a small local area of deformation. A secondary center of subsidence occupies this same area (fig. 20).

The secondary center of contraction, and by inference the associated subsidence, developed after the principal deformation had taken place 2 km farther north, as shown by repeated geodimeter measurements. The five distances shown in figure 22 were measured on February 23 and 25. Three distances in the central part of the caldera lengthened, indicating resumption of expansion. Two distances, both of which cross the area of secondary contraction, shortened. Most of the deformation in the south part of the caldera, then, apparently took place after February 23 and at least partly before February 25. These measurements are completely consistent with the tiltmeter readings (fig. 19) and are the first to suggest that the center of horizontal, as well as vertical, deformation migrates southward during eruptions.

### GROUND DEFORMATION IN THE ERUPTION AREA

#### GROUND CRACKING

In the eruption area, ground cracking was a conspicuous mode of deformation. Compared with the August and October 1968 eruptions, few ground cracks excepting vent fissures themselves were formed or reopened during the February eruption, although many cracks may have gone unnoticed in the dense jungle east of Kane Nui o Hamo. Several new hairline fractures crossed the Chain of Craters Road east of Alae Crater and between Aloi Crater and the eruptive fissure. Remeasurement by tape and leveling at stations designed to monitor movement along preexisting cracks showed negligible displacement at all localities west and southwest of Aloi. Remeasurement, however, showed that the southeast side of a southwest-trending crack near the east rim of Aloi was uplifted 2.6 cm, and 400 m farther east, resurvey of a northeast-trending crack showed no vertical displacement but an opening of 11.6 cm (fig. 23), 1.5 cm of which was due to apparent right-lateral movement. All other newly opened cracks were less than 1 cm wide.

Several wide cracks opened in the area 2–3 km northeast of Kane Nui o Hamo during the eruption, and small volumes of lava erupted from vent D poured into them. We do not know if the drainback cracks were initially vents, as any possible evidence was covered by the flow from vent D. Two long cracks extend from these drainback fissures through jungle to vent F. Trees and ferns were damaged by fume along those cracks, evidence of lava at shallow depths.

A complex set of cracks bounding a new slump block nearly 100 m long and 30 m wide developed on the southwest rim of Alae Crater. The largest crack, about 1.3 m wide, bordered the southeast edge of the slump block and cut the wall of the crater down to the newly

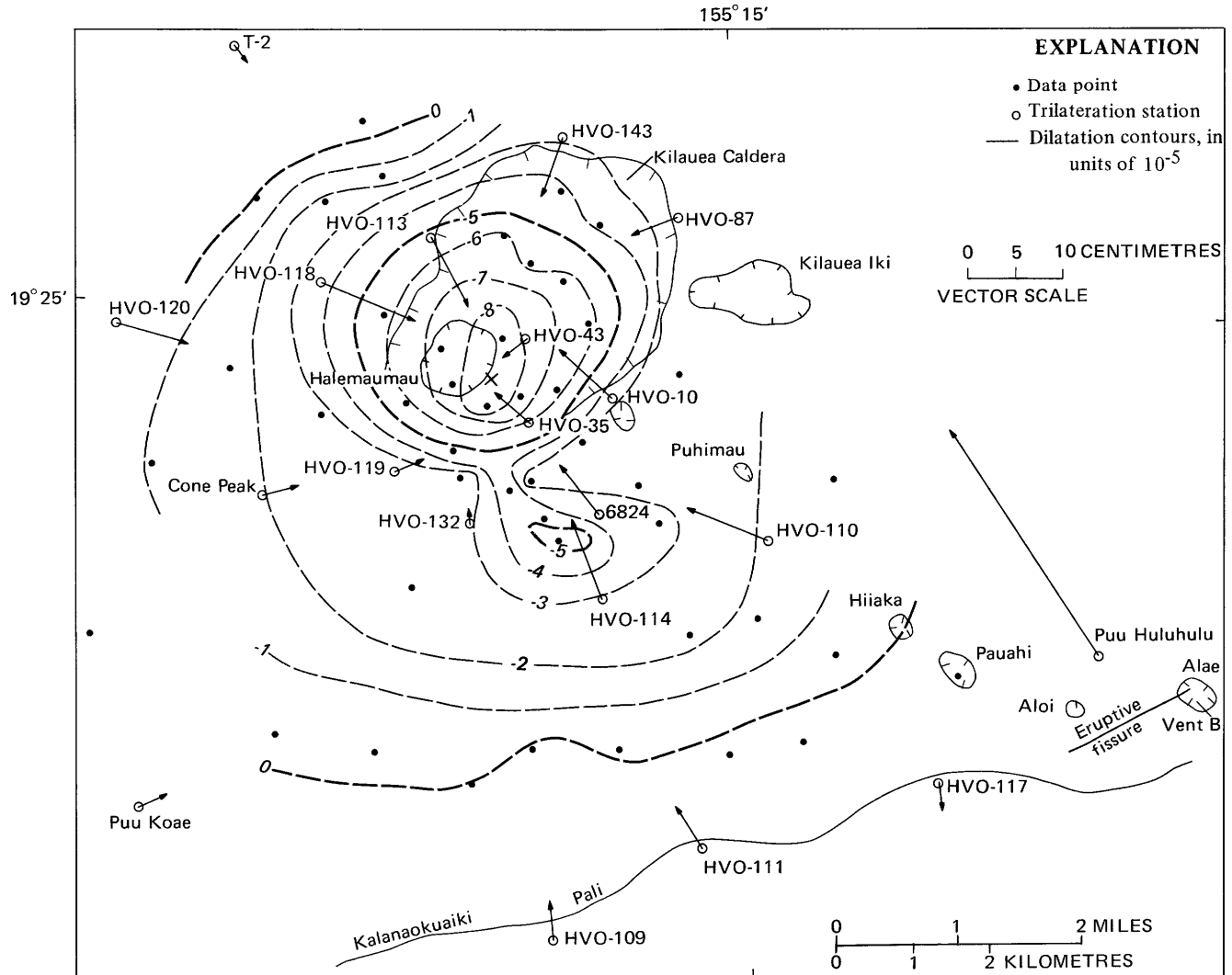


FIGURE 21.—Horizontal displacement (vectors) and dilatational strain (contours) near Kilauea summit and upper east rift between February 11–13 and February 24–27, 1969. Methods same as for figure 5. Note stations Puu Huluhulu and HVO-117, incorporated into trilateration network during this survey period. Cross near east edge of Halemaumau Crater, location of center of deformation used in determination of three-dimensional displacements.

formed lava lake within it (fig. 24). These cracks probably developed from shaking of the unstable rim of the crater during the opening of eruptive fissures, periods of vigorous fountaining, and cascading of lava into the crater. Such ground shaking was readily apparent to observers on the rim of Alae early in the eruption only a short while before the cracks must have formed. The slump block continued to subside and move slowly craterward over the next 6 months; it would have eventually fallen if Alae had not filled with lava in the fall of 1969 (Swanson and others, 1972).

#### HORIZONTAL DEFORMATION

The upper east rift zone underwent substantial horizontal deformation during the eruption, judged by the displacement of almost 29 cm at Puu Huluhulu (fig. 21).

This displacement was almost normal to the trend of the eruptive fissures and probably largely reflects the opening of the fissures and associated cracks, although uplift along the fissure zone (fig. 20) contributed to minor displacement. The cumulative width of new cracks and fissures is unknown but certainly more than 29 cm. Some of the new opening must have been accommodated by closing of preexisting cracks between the fissure zone and Puu Huluhulu, by southeastward displacement south of the fissure zone, by accumulation of elastic strain (probably of minor importance), or by a combination of these factors. Consideration of the structure of Kilauea's south flank and how it has responded to past rift eruptions suggests that the area south of the fissure zone was displaced southeastward by several tens of centimetres (Swanson and others, 1976).

The character of ground displacement north and northwest of Puu Huluhulu is not known. Station HVO-87 was apparently unaffected by the opening of the new fissures, for its displacement is consistent with the summit deformation. Numerous pre-1969 cracks and fissures occur north of Puu Huluhulu; closing of these cracks may have taken up much of the displacement recorded at Puu Huluhulu. This situation contrasts markedly with that south of the east rift zone, where strains are transmitted many kilometres southeastward during intrusive and ground-cracking events along the rift (Koyanagi and others, 1972; Swanson and others, 1976).

Station HVO-117, only about 1.7 km along strike from the nearest active vent, was displaced less than 3 cm away from the projected fissure (fig. 21). This small displacement shows that the deformation died out rapidly beyond the end of the fissure zone, a conclusion confirmed from examination of crack measuring stations.

#### VERTICAL DEFORMATION

The east rift zone was uplifted sharply near the eruption site. Maximum measured uplift was 90.6 cm at the bench mark closest (450 m) to the fissures between Alae and Makaopuhi Craters (fig. 20). The uplift is narrow and very abrupt, gradients being 35 cm/km at the Makaopuhi tiltmeter station and greater than 50 cm/km near Alae.

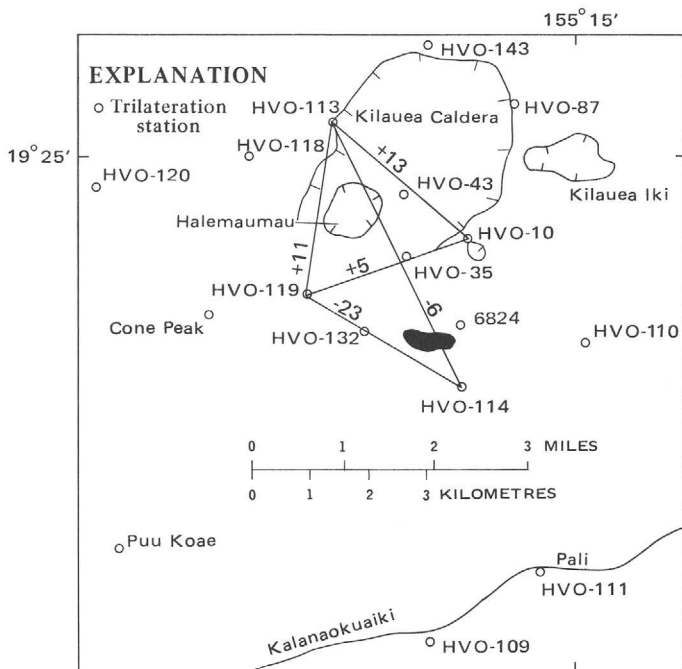


FIGURE 22.—Change in length (in mm) of five geodimeter lines between February 23 and 25, 1969, during the eruption. Distances involving station HVO-114 contracted, others lengthened. Shaded area indicates subsidiary center of contraction; see figure 21.

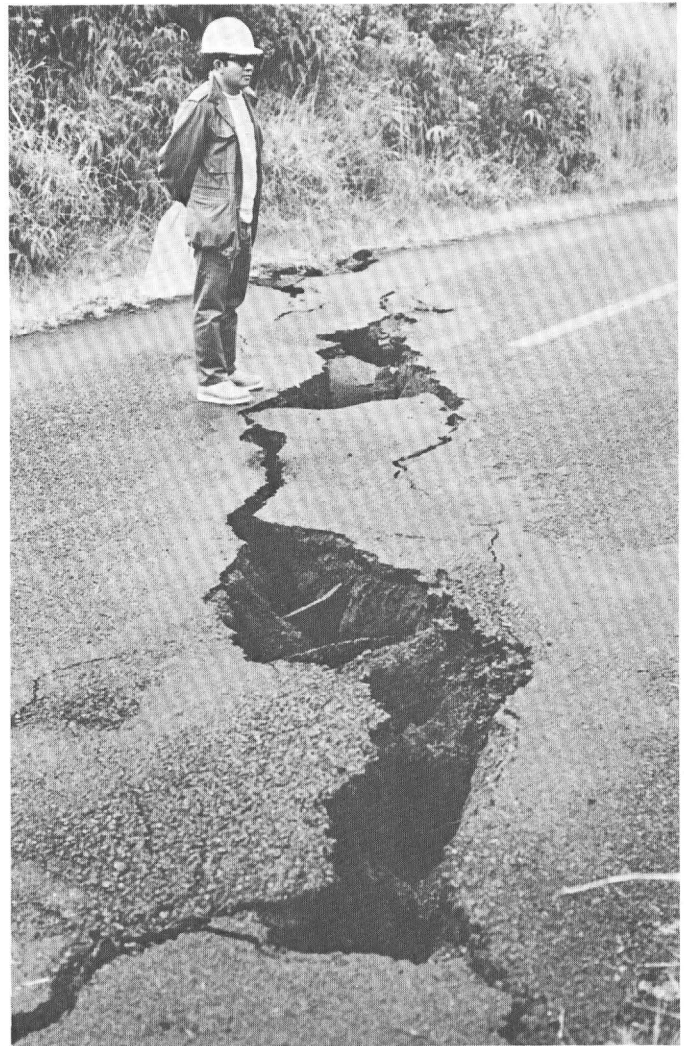


FIGURE 23.—New opening of preexisting crack cutting Chain of Craters Road 400 m east of Aloi Crater, near eruptive fissure. Measured amount of opening at a station just off road is 11.6 cm. Note roots extending across crack and remnant of an asphalt patch used to cover crack after it opened in December 1965 (Fiske and Koyanagi, 1968). View toward southwest.

Neither the shape of the uplift nor the location of its crest is known; contours were drawn (fig. 20) by assuming that the uplift is centered over the fissure zone and elongate along it. The location of the crest is most speculative, but the assumed trend parallel to the fissures is supported by the azimuths of tilt at Makaopuhi (fig. 20) and horizontal displacement at Puu Huluhulu (fig. 21).

The origin of this uplift is conjectural. It may largely reflect intrusion of magma at very shallow depths as sills and nearly vertical dikes. Uplift along a fault just south of the fissure zone could explain the meager displacement data, as could uplift associated with south-dipping dikes if the crest of the uplift were south of the



FIGURE 24.—Master crack bounding slump block that formed along south edge of Alae Crater during February 1969 eruption. Note subsidence and displacement toward crater.

fissure zone. Jackson, Swanson, Koyanagi, and Wright (1975) examined these possibilities for the August 1968 eruption and found that emplacement of either a dike dipping about  $80^\circ$  southward or a vertical dike accompanied by faulting south of the fissure could account for the observed displacements.

The eruption-related uplift, though abrupt and large, was only the culmination of a 5-month period of steady uplift in the vicinity of Makaopuhi (fig. 4). For example, the bench mark most displaced (90.6 cm) during the eruption had been raised at least 9.2 cm between October 10, 1968 and February 5, 1969. The final location of preeruption uplift may have been close to that of the February fissure zone on Kane Nui o Hamo (figs. 1 and 4B).

Two bench marks along the Chain of Craters Road within 100 m of the active fissure subsided 10 and 13 cm, respectively, and one in the same area was uplifted only 2 cm. These bench marks are within the area of the keystone graben shown in figure 20. These displacements suggest a zone of local subsidence superimposed on the larger area of uplift. Most of the subsidence took place within a distance of about 60 m between two permanent survey stations on the highway. No new cracks cut the pavement between these stations, and a careful check revealed no spurious disturbances of the stations themselves.

We interpret this area of subsidence to be part of a keystone graben or half graben that formed along the

crest of the overall uplift. Where crossed by the level line, the north edge of this graben was expressed as an abrupt monoclinical flexure. The south edge of the graben could not be examined, as it was covered with new lava. Graben faults may have formed elsewhere along the fissure trend, although none was seen in the dense forest or beneath the new lava. Keystone grabens or elongate zones of subsidence commonly, if not always, develop along eruptive fissures on the east rift zone; they have been described or figured by Macdonald and Eaton (1964, p. 105–107) for the 1955 eruption, by Fiske and Koyanagi (1968, fig. 8) for the December 1965 eruption, and by Jackson, Swanson, Koyanagi, and Wright (1975) for the August 1968 eruption.

#### DEPTH TO SUMMIT MAGMA RESERVOIR

Inflation and deflation of the summit region presumably reflect changes of magmatic pressure within the complex magma reservoir. Studies of ground displacement provide clues on depths to the pressure source, generally considered to be the upper part of this reservoir system. Such studies at Kilauea have traditionally used elastic models, in particular, the point-source model of Mogi (1958), to arrive at depths in the range 2 to 4 km (Eaton, 1962; Fiske and Kinoshita, 1969; Jackson and others, 1975). Different models yield different depths, and each model is a greatly oversimplified version of the real reservoir system. It is therefore desirable to check this range in model depths by an independent method.

In this section we compare source depths derived from five models, four elastic and one plastic, and depths determined by a graphic method involving derivation of three-dimensional ground displacements. The February eruption and preceding inflation provide the best test to date of the five models, for no reliable horizontal displacement data were available for earlier periods (those used by Fiske and Kinoshita (1969) involved only linear strains in a floating network). For the first time, vertical and horizontal models can be directly compared.

In 1973, while this paper was being written, a 1.26-km-deep test hole was drilled at a site 1.1 km due south of the south rim of Halemaumau (fig. 1), but no magma reservoir was penetrated (Zablocki and others, 1974). The site is near the west edge of a commonly active deformation center (fig. 3, area B). At this location, then, the magma reservoir system is deeper than 1.26 km, although it is possible that parts extend above this level nearby.

#### ELASTIC AND PLASTIC PSEUDOCAMBER MODELS

Depths to source were estimated by using the elastic models for a point source of constant displacement

(Mogi, 1958), a point source of the thrust-pressure type (Yokoyama, 1971), a vertical line source (Walsh and Decker, 1971), a vertical plug source (Dieterich and Decker, 1975), and a plastic pseudo-chamber source (Davis and others, 1974) for the period of summit inflation (figs. 4B and 5B) before the eruption. This period was chosen because the data show less scatter when plotted relative to distance from a possible source epicenter than the data for deflation accompanying the eruption.

The fit of theoretical model curves to the vertical displacement, horizontal displacement (radial component, see table 5), and tilt<sup>1</sup> data is shown on figure 25. Fairly good fits to the horizontal-displacement data (fig. 25B) can be made for all five model curves and to the tilt data (fig. 25C) for the Mogi point-source and the vertical line source curves. Only the Mogi point source, the vertical plug, and the plastic pseudo-chamber models provide adequate fits to the leveling data (fig. 25A) unless sizable arbitrary adjustments are added to the leveling datum (Fiske and Kinoshita, 1969; Jackson and others, 1975).

None of the models gives internally consistent source depths when considering all three types of deformation measurements (fig. 26). This is clearly seen when comparing discrepancies in source depths between the vertical and horizontal displacement models calculated for a vertical plug source whose top is located at a depth of 1 km (fig. 27). A good fit to the vertical deformation data can be made for a focal depth of about 1 km, but the far-field horizontal displacements are too large and the maximum displacements occur too far from the chosen source epicenter for this focal depth. A source depth of about 2.1 km (dashed curve) is required to match the horizontal displacement data of figure 27. This kind of discrepancy is true for all models considered in this paper. The wide scatter of source depths indicates that none of the deformation models now available adequately represents the true configuration of the source. This is not surprising in view of idealized assumptions for the models and the demonstrated complexity of the surface deformation. It is clear that these models can be used only to provide crude estimates of the range in source depths.

### THREE DIMENSIONAL DISPLACEMENT METHOD

The source depth can be estimated independently by using the three-dimensional displacement of stations within the geodetic networks. These displacements are derived by vector addition of the horizontal and vertical components of displacement at each survey station. Pro-

jection of the three-dimensional displacement vector from each station to a point directly beneath the center of surface deformation yields the depth to the pressure source (fig. 28), assuming that the center of surface deformation is directly above the source and that the displacement path is not refracted between source and survey station. The first assumption seems reasonable for the summit area, but the second is probably invalid to some unknown degree owing to the effect of the free ground surface on the stress field.

Depths were graphically determined in this way for the December 1968–February 1969 inflation (fig. 28A) and the February 1969 deflation (fig. 28B), assuming the centers of the deformation were located as shown in figures 5B and 20. Two alternative depths were derived, the shallower by using the measured horizontal displacement, the deeper by using only the radial component of displacement. Unless otherwise noted, the depths discussed in this section are those derived from the radial component. Vertical displacements not measured directly were estimated from the contour maps (figs. 4B and 20).

The results (fig. 28; table 5) indicate a wide range of depths. The average of the 26 radially derived depths (omitting station HVO-132 during the deflation) is 2.0 km (1.6 km for the inflation, 2.5 km for the deflation). This average agrees with the various elastic and plastic model depths to the extent that the pressure source is shallow. The average depth, however, is less than that predicted by any of the horizontal-displacement models except the vertical plug source (fig. 26), because the horizontal displacements are larger than those predicted by most of the models. If depths based on the measured horizontal displacement, not the radial component, are used, the average becomes shallower and the discrepancy with the models is increased.

The average calculated source depth during the inflation is about 0.9 km less than that during the deflation. This difference, if real, may indicate that the processes of filling and emptying the reservoir follow different pathways.

The migration of deformation centers with time (figs. 3 and 19) proves that the reservoir system is complex, and some of this complexity is probably reflected by the scatter of apparent source depths in figures 26 and 27. Another critical factor that contributes to the scatter is the unknown but finite size of the reservoir. Realistically, the reservoir has both breadth and depth, and some of the scatter in figure 28 may partly define these dimensions.

### DISCUSSION AND SPECULATION

Much quantitative information on ground deformation at Kilauea has been acquired over the past several

<sup>1</sup>Yokoyama (1971), Dieterich and Decker (1975), and Davis, Hastie, and Stacey (1974) give no theoretical tilt curves.

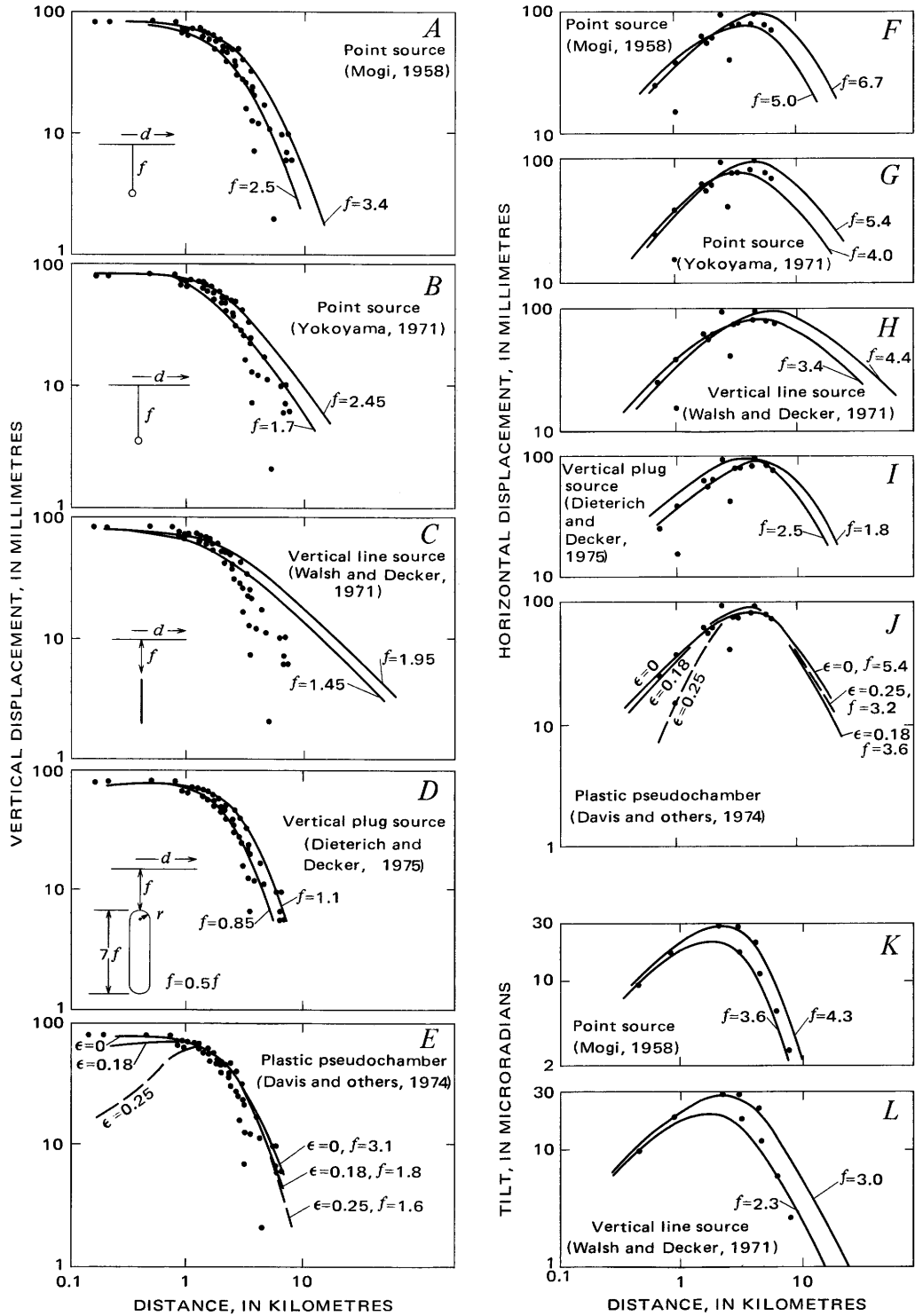


FIGURE 25.—Elastic and plastic pseudo-chamber model curves compared with measured vertical and horizontal displacement and ground tilt for November 1968–February 1969 summit inflation relative to horizontal distance  $d$  from epicenter of source to a datum point along the ground surface. A–E, Vertical displacement models, data from figure 4B. F–J, Horizontal displacement models, data from table 5. K–L, Tilt models, data from figure 4B. Source depth  $f$  equals depth in kilometres to point source, tops of vertical line and vertical plug sources, or center of ellipsoid of plastic pseudo-chamber model.  $\epsilon$ , ellipticity of plastic pseudo-chamber model;  $r$ , cavity radius. Solid dot, data point.

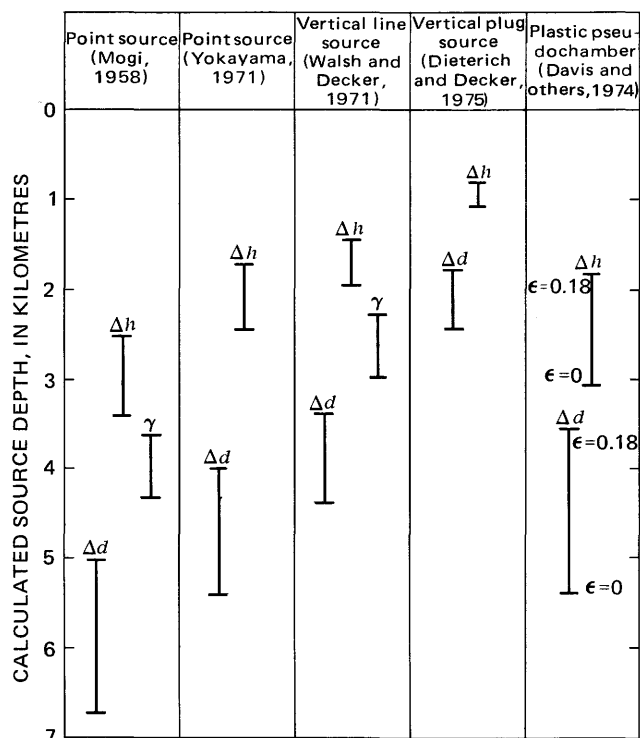


FIGURE 26.—Range of calculated source depths for deformation models of figure 25.  $\Delta d$ , horizontal displacement model;  $\Delta h$ , vertical displacement model;  $\gamma$ , tilt model.

years with two broad aims in mind: to provide both empirical and theoretical bases for predicting future eruptions, and to help define the internal structure and plumbing of the volcano. In this section we discuss how the data collected before and during the February eruption contribute to these two aims.

#### ERUPTION PREDICTION BY USING DEFORMATION DATA

In retrospect it is clear that by mid-February an eruption was imminent. At the time, however, we felt that it was still some weeks away. Our judgment was based on the degree of deformation of the summit area: the tilt, uplift, and strain were not at a level as high as before the flank eruptions of the preceding August and October. It is likely that structural adjustments within the volcano resulting from these eruptions were sufficiently large to require changes in the base levels used for comparing the deformation data. Some of those adjustments may have been permanent, some short-lived. We are at present unable to recognize or fully evaluate such changes, and until we can, only the crudest kind of prediction can be made from the deformation data alone.

There are favorable signs, though. For example, each of the five distances in the weekly strain monitor (the same distances shown in fig. 22) lengthened about as much between October 1968 and February 1969 as between February and late May, when the 1969–71 Mauna

TABLE 5.—Displacements of survey stations and depths to pressure source (magma reservoir) beneath Kilauea Caldera before and during February eruption  
[See text for further explanation]

	Station	Distance (km) from center of deformation	Vertical displacement (cm)	Total horizontal displacement (cm)	Radial component of horizontal displacement (cm)	Source depth (km)	
						Using total horizontal displacement	Using radial horizontal displacement
Inflation, December 1968– February 1969 (see fig. 4B and 5B)	HVO-132	0.7	7.9	2.5	2.5	2.2	2.2
	HVO-119	1.0	7.1	2.5	1.5	3.0	4.6
	HVO-35	1.0	6.8	5.0	3.8	1.4	1.9
	6824	1.7	6.0	6.2	6.2	1.7	1.7
	HVO-43	1.9	5.1	7.0	5.5	1.4	1.8
	HVO-10	2.0	4.8	7.5	6.2	1.4	1.6
	HVO-114	2.4	5.0	9.4	9.4	1.2	1.2
	Cone Peak	2.8	3.5	6.7	4.0	1.5	2.4
	HVO-113	3.1	2.5	7.7	7.5	1.0	1.1
	HVO-118	3.2	2.0	10.0	7.5	.7	.8
	HVO-87	4.3	1.5	8.0	7.8	.9	1.0
	HVO-143	4.6	1.6	9.5	9.5	.6	.6
	HVO-111	5.8	1.0	8.0	8.0	.6	.6
	HVO-109	6.4	1.0	7.5	7.5	.8	.8
	Deflation during February 1969 eruption (see figs. 20 and 21)	HVO-43	0.6	11.5	2.9	2.9	2.1
HVO-35		.8	10.5	4.9	4.8	1.8	1.8
HVO-10		1.5	7.8	7.6	6.8	1.6	1.8
HVO-113		1.9	5.8	8.0	8.0	1.4	1.4
HVO-119		1.9	9.4	3.3	3.1	5.2	5.5
HVO-132		2.0	10.0	.8	.8	>10	>10
6824		2.3	8.7	6.6	6.6	2.9	2.9
HVO-118		2.8	4.9	10.5	10.3	1.3	1.4
HVO-87		3.1	3.5	5.3	4.8	2.0	2.2
HVO-143		3.2	3.0	6.2	6.2	1.8	1.8
HVO-114		3.3	7.2	8.6	8.6	2.8	2.8
Cone Peak		3.6	5.6	3.3	3.2	5.9	6.0
HVO-110	4.2	1.2	9.2	8.7	.7	.8	

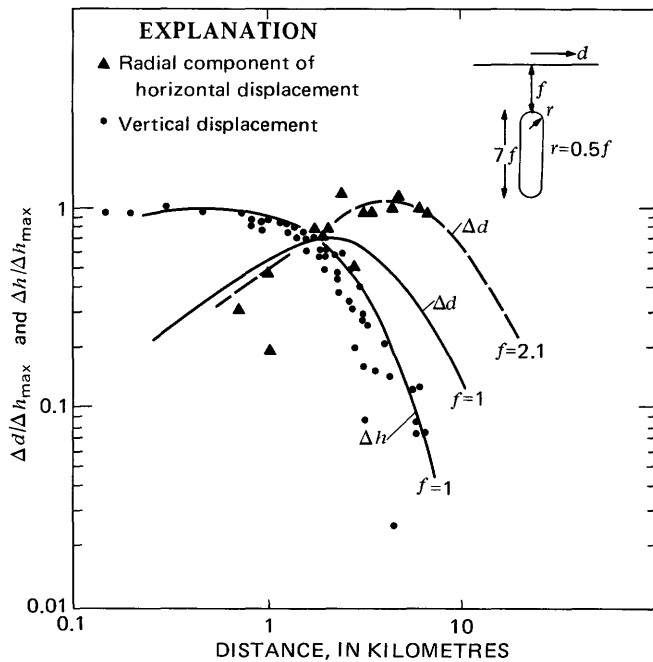


FIGURE 27.—Field data from figures 4B and 5B for late 1968–February 1969 summit inflation compared with vertical and horizontal displacement model curves for a vertical plug source (Dieterich and Decker, 1975) whose top surface is located 1 km beneath the ground surface, relative to horizontal distance  $d$  from epicenter of source to a data point along ground surface.  $\Delta d$ , horizontal displacement;  $\Delta h$ , vertical displacement. Dashed line, horizontal displacement curve that fits field data for a source depth of 2.1 km. Symbols as in figure 25.

Ulu eruption began (fig. 29 and table 6). In fact, the outbreak in May was anticipated partly on the basis of this information. Each distance extended differently, but each had repeated to within 12 percent the same degree of extension during both periods of inflation. We do not suggest that this is a foolproof or even consistent predictive tool, in part because of the base-level ambiguity discussed. Nonetheless, such studies show considerable promise at Kilauea.

#### MAKAOPUHI MAGMA RESERVOIR

Evidence summarized below suggests that a magma reservoir was present near Makaopuhi Crater before the February 1969 eruption.

1. The area near Makaopuhi was uplifted more than 10 cm between October 10, 1968 and early February 1969 (fig. 4C). Most of this uplift took place after late November and cannot be ascribed to aftereffects of the October eruption. Furthermore, the center of uplift shifted from south to north of Makaopuhi (compare figs. 4A and 4B), indicating a mobile source of deformation.

2. The daily number of earthquakes near Makaopuhi gradually increased between November and February, suggesting stress buildup reasonably attributable to injection of magma into the rift zone.

3. The near-absence of earthquakes between the summit and vent areas during the eruption (fig. 17) suggests that a virtually unobstructed conduit was present before the eruption began. Such a conduit could have periodically tapped magma from the central reservoir beneath the caldera and transported it to the Makaopuhi storage area months before the eruption.

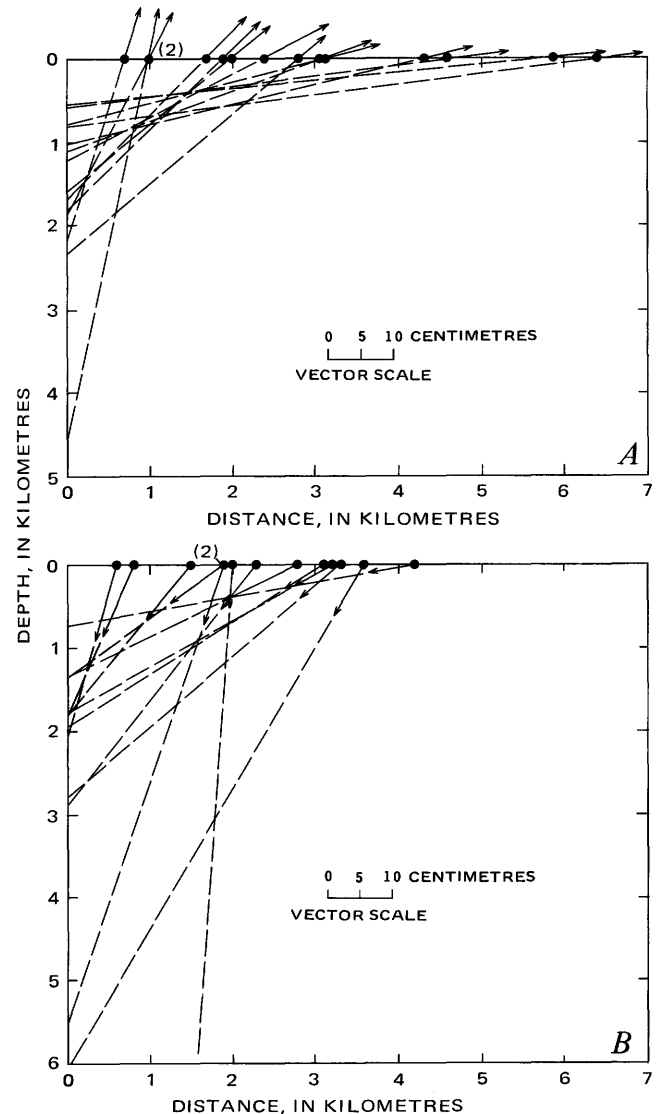


FIGURE 28.—Source depths derived from three-dimensional displacements. A, December 1968–February 1969 inflation. B, February 1969 deflation. Radial components of horizontal displacement are added to vertical displacements at each indicated station to give three-dimensional displacement (vectors). Assuming center of deformation directly above source and path of displacement not refracted, projection of vector line (dashed line) to point below center of deformation gives source depth. Components of displacement and source depths listed in table 5. Data and station locations shown in figures 4B, 5B, 20, and 21. Several outlying stations omitted from one or both diagrams and from table 5, because their vertical displacements are unknown or inconsistent with overall summit deformation.

4. Seismicity was strongest in the Makaopuhi-Alae area (figs. 6, 16B) just before the eruption, as if magma stored there were forcibly working its way to the surface. Only when the summit began to rapidly deflate did caldera earthquakes become frequent.

5. The volume of erupted lava (about  $20 \times 10^6 \text{m}^3$ ) is significantly more than that of summit subsidence, whether computed by integration of the vertical displacement map or by Eaton's method (1962) for focal depths of 4 km or less. If the volume of subsidence is roughly equivalent to the volume of magma that left the summit reservoir, then a secondary source of magma within the rift zone is called for.

Similar reasoning led Jackson, Swanson, Koyanagi, and Wright (1975) to infer a magma reservoir in the Makaopuhi area before the October 1968 eruption. This reservoir system may have operated over a period of more than 5 months in late 1968 and early 1969. Leveling data between 1966 and early 1968 further suggests that deformation was taking place near Makaopuhi during that time (Hawaiian Volcano Observatory, unpublished data, 1968).

Shallow storage reservoirs would be favorable places for comparatively rapid cooling of magma after injection into the rift zone. Such cooling is necessary to ac-

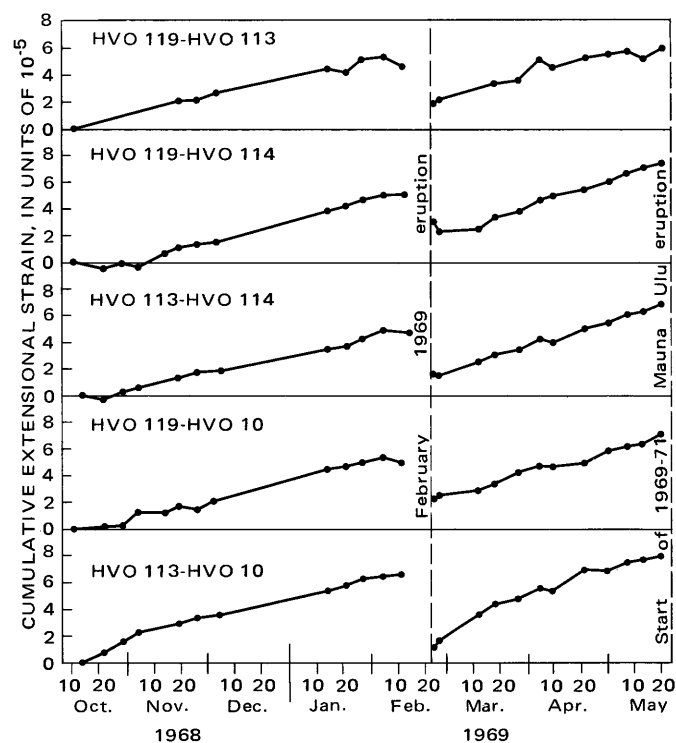


FIGURE 29.—Cumulative extension for five geodimeter lines in Kilauea Caldera between mid-October 1968 and mid-May 1969. Extensional strain arbitrarily set at 0 for initial measurement. Locations of measured lines shown in figure 22.

TABLE 6.—Cumulative extension of distances in summit strain monitor for two periods of inflation, Kilauea Volcano

Distance	Approximate length (m)	Cumulative extension, units of $10^{-5}$	
		Oct. 12, 1968–Feb. 12, 1969	Feb. 24–May 20, 1969
HVO113–HVO10	3,097	6.56	6.83
HVO119–HVO10	2,893	4.94	4.80
HVO113–HVO114	5,128	4.74	5.23
HVO119–HVO114	3,070	5.15	5.18
HVO119–HVO113	3,155	4.75	4.12

count for the numerous differentiated and hybrid lava flows on Kilauea's east rift zone (Wright and Fiske, 1971). For example, some lava erupted during October 1968 shows evidence of pyroxene fraction, and this may have occurred in the storage system near Makaopuhi (Jackson and others, 1975; Wright and others, 1975). The chemical compositions of all February 1969 lava samples also indicate mixing with a somewhat cooler differentiated magma (Wright and others, 1975), although phenocrysts of pyroxene and plagioclase are relatively uncommon (table 3). We conclude from this that most of the 1969 magma was held in the Makaopuhi reservoir system for a comparatively short time before erupting, perhaps 4 months, the duration of the pre-eruptive period.

The shallow focal depths (generally much less than 5 km) of earthquakes in the Makaopuhi area suggests that the magma reservoir is located well within the edifice of Kilauea itself, whose base is probably about 8–10 km below sea level (Hill, 1960). The repeated long-term presence of magma within such a high-level reservoir must tend to weaken the roofrock through stopping, melting, distension as the reservoir fills and changes shape, and related processes. Weakening of the roof may eventually cause collapse and formation of a pit crater. The numerous pit craters on the upper and lower east rift zone (pl. 1; Macdonald and Eaton, 1964, pl. 1) may have formed above such local reservoirs. The largest pit crater on the east rift zone, the double crater Makaopuhi, suggests the presence of a large, shallow reservoir in this general area during much of the past few hundreds or thousands of years.

The minimum volume of the present reservoir beneath the Makaopuhi area can be estimated as the volume of erupted lava minus the volume of summit subsidence, assuming a closed system and a one-to-one correspondence between magma and deformation volumes. The assumption of a closed system seems reasonable, as there was no detected ground deformation and very little seismicity along the east rift zone between the summit and eruption areas (fig. 17). The second assumption cannot be tested at present.

The minimum reservoir volume calculated in this

way (after adjusting the volume of summit subsidence to  $5 \times 10^6 \text{m}^3$  to accommodate inflation between leveling surveys) is  $15 \times 10^6 \text{m}^3$ , approximately equivalent to a sphere 300 m in diameter. This estimate is probably unreasonably small, for total emptying of the reservoir is unlikely, and measured uplift and dilation near Makaopuhi during the eruption was substantial, implying a larger, possibly much larger reservoir volume.

Another way to estimate the minimum reservoir volume is to assume a constant magma supply to Kilauea of  $9 \times 10^6 \text{m}^3/\text{month}$  (Swanson, 1972). This rate would have accounted for  $36 \times 10^6 \text{m}^3$  of magma throughout the 4-month-long period of preeruptive inflation. The summit swelled only a little more than  $2.4 \times 10^6 \text{m}^3$  during this time, however, leaving a difference of nearly  $34 \times 10^6 \text{m}^3$  (equivalent to a sphere of about 400 m in diameter) to be accounted for by the Makaopuhi storage system. The geodetic networks along the rift zone are inadequate for computation of deformation volumes to check this estimate. It nonetheless seems more reasonable than the lower estimate of  $15 \times 10^6 \text{m}^3$ , because it can account for at least part of the observed volume of uplift during the eruption.

These calculations suggest minimum volumes comparable to, or slightly less than, those of many pit craters on the east rift zone. As these pit craters contain notably small amounts of talus, they cannot have grown greatly through mass wasting following their formation. Their dimensions, then, may be crude guides to the size and shape of underlying reservoirs, although characterization of a reservoir as a simple sphere is certainly oversimplified.

#### NATURE OF MAGMA CONDUIT BETWEEN SUMMIT AND ERUPTION SITE

The virtual absence of earthquakes between the summit and eruption areas before and during the eruption suggests that a nearly unobstructed magma conduit connected the two areas, and this is implied by the gradual filling of the Makaopuhi reservoir before the eruption. Such a conclusion holds for the August and October 1968 east rift eruptions (Jackson and others, 1975). For all three eruptions, the first earthquakes were generated beneath the vent area, not the summit, and almost no earthquakes occurred at intermediate locations. From this timing, we can infer that increased fluid pressure caused dikes to split upward from the conduit system at points of weakness, such as the Makaopuhi reservoir in October 1968 and February 1969 or the site of a temporary blockage of the conduit near Hiiaka Crater in August 1968.

It appears to us that many east rift eruptions are not

fed directly by dikes that forcibly wedge themselves all the way downrift from the summit storage system to the site of eruption. Some eruptions may indeed be fed by such dikes (Fiske and Jackson, 1972); in fact, the open conduits themselves may have originated as long, blade-like dikes extending downrift from the summit. The evidence presented here, however, suggests that many east rift eruptions are fed by much less extensive dikes that intrude upward from a fluid-filled conduit system interconnected with the summit reservoir. Once started, these dikes can propagate at shallow depths, possibly by hydrofracturing, for many kilometres along the rift zone beyond the terminus of the supply conduits; clearly this took place during the eruptions of August and October 1968 (Jackson and others, 1975) and February 1969.

Seismic evidence from all well-documented east rift eruptions supports the concept of a fluid core transmitting magma to a point where diking is initiated. Even the 1955 and 1960 eruptions, which took place 30 km or more from the summit, were not immediately preceded by a swarm of earthquakes that moved downrift as if at the leading edge of a dike; rather, virtually all earthquakes occurred in the summit and eruption areas only, supporting a fluid connection between the two areas. It was probably in such conduits and local reservoirs intersected by them that much of the mixing of magmas, documented by Wright and Fiske (1971) for the 1955, 1960, and other east rift eruptions, took place.

Studies of 20th century horizontal ground displacement along the east rift zone (Swanson and others, 1976) indicate that dilation is at a maximum near the site of eruption and decreases markedly uprift, consistent with forceful intrusion of magma in the immediate eruption area only.

The postulated open conduits were likely initiated as long dikes at some unknown time in the past but probably have so markedly enlarged or changed shape by such processes as stoping and melting that they may no longer be considered dike-like. Enlargement of such conduits at structurally favorable sites such as the area of intersection of the Koae fault system (Duffield, 1975) and the east rift zone may be one of the prime factors leading to the formation of shallow reservoirs and subsequently to pit craters.

At times, a conduit can apparently become plugged, perhaps by wallrock caving or magma solidification. This has taken place several times since 1970 (Hawaiian Volcano Observatory, unpub. data, 1974). A partial blockage may have formed near the intersection of the Koae fault system and the east rift zone during the violent ground-cracking and seismic event in De-

ember 1965 (Fiske and Koyanagi, 1968) to account for: (1) the unusually long period (32 months) before the next rift eruption (August 1968); (2) the intervening 1967–68 summit eruption, which relieved some of the fluid pressure accumulated within the volcano, and (3) the accompanying very slow leakage of magma into the Makaopuhi reservoir, as documented by leveling surveys at the time. The August 1968 eruption and ground cracking may have taken place near the postulated blockage, destroying it so that once again magma had full access to the Makaopuhi reservoir, as the evidence for the succeeding October 1968 and February 1969 eruptions suggests. Another temporary blockage occurred in the same area in May 1970, briefly interrupting an eruption farther downrift at Mauna Ulu. This blockage led to a brief seismic crisis and shallow intrusion of magma uprift from the blockage before the conduit system was reopened and the eruption resumed (Duffield and others, 1975; Endo, 1971).

We suspect that, among Hawaiian volcanoes, a fluid core is not unique to the east rift zone of Kilauea, but characterizes most rift zones during the shield-building stage. Such cores have not been recognized in the deeply eroded shields, possibly because they lie below sea level. All that is seen in the subaerial parts of eroded Hawaiian shields are steeply dipping dikes, many of which may, in our interpretation, be rooted in a deeper conduit.

## REFERENCES CITED

- Davis, P. M., Hastie, L. M. and Stacey, F. D., 1974, Stresses within an active volcano—with particular reference to Kilauea: *Tectonophysics*, v. 22, p. 355–362.
- Dieterich, J. H. and Decker, R. W., 1975, Finite element modeling of surface deformation associated with volcanism: *Jour. Geophys. Research*, v. 80.
- Duffield, W. A., 1975, Structure and origin of the Koaie fault system, Kilauea Volcano, Hawaii: U.S. Geol. Survey Prof. Paper 856, 12 p.
- Duffield, W. A., Jackson, D. B. and Swanson, D. A., 1975, The shallow, forceful intrusion of magma and related ground deformation at Kilauea Volcano, May 15–16, 1970: *Bull. Volcanol.* (in press).
- Eaton, J. P., 1959, A portable water-tube tiltmeter: *Seismol. Soc. America Bull.*, v. 49, p. 301–316.
- , 1962, Crustal structure and volcanism in Hawaii: *Am. Geophys. Union Mon.* 6, p. 13–29.
- Endo, E. T., 1971, Focal mechanism for the May 15–18, 1970, shallow Kilauea earthquake swarm: San Jose State College, San Jose, Calif., M.S. thesis.
- Fiske, R. S., and Jackson, E. D., 1972, Orientation and growth of Hawaiian volcanic rifts: the effect of regional structure and gravitational stresses: *Royal Soc. London Proc., ser. A.*, v. 329, p. 299–326.
- Fiske, R. S., and Kinoshita, W. T., 1969, Inflation of Kilauea Volcano prior to its 1967–1968 eruption: *Science*, v. 165, p. 341–349.
- Fiske, R. S. and Koyanagi, R. Y., 1968, The December 1965 eruption of Kilauea Volcano, Hawaii: U.S. Geol. Survey Prof. Paper 607, 21 p.
- Hill, D. P., 1969, Crustal structure of the island of Hawaii from seismic-refraction measurements: *Seismol. Soc. America Bull.*, v. 59, p. 101–130.
- Jackson, D. B., Swanson, D. A., Koyanagi, R. Y., and Wright, T. L., 1975, The August and October 1968 flank eruptions of Kilauea Volcano, Hawaii: U.S. Geol. Survey Prof. Paper 890, 33 p.
- Kinoshita, W. T., Koyanagi, R. Y., Wright, T. L., and Fiske, R. S., 1969, Kilauea Volcano—The 1967–68 summit eruption: *Science*, v. 166, p. 459–468.
- Kinoshita, W. T., Swanson, D. A. and Jackson, D. B., 1974, The measurement of crustal deformation related to volcanic activity at Kilauea Volcano, Hawaii, in Civetta, L., Gasparini, P., Luongo, G., and Rapolla, A., eds., *Physical Volcanology*, Elsevier, Amsterdam, p. 87–115.
- Koyanagi, R. Y., and Endo, E. T., 1971, Hawaiian seismic events during 1969: U.S. Geol. Survey Prof. Paper 750–C, p. C158–C164.
- Koyanagi, R. Y., Swanson, D. A., and Endo, E. T., 1972, Distribution of earthquakes related to mobility of the south flank of Kilauea Volcano, Hawaii, in *Geological Survey research 1972*: U.S. Geol. Survey Prof. Paper 800–D, p. 89–97.
- Koyanagi, R. Y., Takeguchi, S. A., and Kinoshita, W. T., 1970, Hawaiian Volcano Observatory Summary 53, 26 p.
- Macdonald, G. A. and Eaton, J. P., 1964, Hawaiian volcanoes during 1955: U.S. Geol. Survey Bull. 1171, 170 p.
- Mogi, Kiyoo, 1958, Relations between the eruptions of various volcanoes and the deformation of the ground surfaces around them: *Tokyo Univ. Earthquake Research Inst. Bull.*, v. 36, p. 99–134.
- Moore, J. G., and Koyanagi, R. Y., 1969, The October 1963 eruption of Kilauea Volcano, Hawaii: U.S. Geol. Survey Prof. Paper 614–C, 13 p.
- Moore, J. G. and Krivoy, H. L., 1964, The 1962 flank eruption of Kilauea Volcano and structure of the east rift zone: *Jour. Geophys. Research*, v. 69, p. 2033–2045.
- Peck, D. L., Wright, T. L. and Moore, J. G., 1966, Crystallization of tholeiitic basalt in Alae lava lake, Hawaii: *Bull. Volcanol.*, v. 29, p. 629–655.
- Peck, L. C., 1964, Systematic analysis of silicates: U.S. Geol. Survey Bull. 1170, 89 p.
- Shaw, H. R., Kistler, R. W., and Evernden, J. F., 1971, Sierra Nevada plutonic cycle—Part II, tidal energy and a hypothesis for orogenic-epirogenic periodicities: *Geol. Soc. America Bull.*, v. 82, p. 869–896.
- Swanson, D. A., 1972, Magma supply rate at Kilauea Volcano, 1952–1971: *Science*, v. 175, p. 169–170.
- Swanson, D. A., Duffield, W. A. and Fiske, R. S., 1976, Displacement of the south flank of Kilauea Volcano: the result of forceful intrusion of magma into the rift zones: U.S. Geol. Survey Prof. Paper, in press.
- Swanson, D. A., Duffield, W. A., Jackson, D. B. and Peterson, D. W., 1972, The complex filling of Alae Crater, Kilauea Volcano, Hawaii: *Bull. Volcanol.* v. 36, p. 105–126.
- Swanson, D. A., Jackson, D. B., Duffield, W. A. and Peterson, D. W., 1971, Mauna Ulu eruption, Kilauea Volcano: *Geotimes*, v. 16, no. 5, p. 12–16.
- Thompson, R. N., and Tilley, C. E., 1969, Melting and crystallization relations of Kilauean basalts of Hawaii: The lavas of the 1959–60 Kilauea eruption: *Earth and Planetary Sci. Letters*, v. 5, p. 469–477.
- Walsh, J. B., and Decker, R. W., 1971, Surface deformation associated with volcanism: *Jour. Geophys. Research*, v. 76, p. 3291–3302.
- Wright, T. L., and Fiske, R. S., 1971, Origin of the differentiated and hybrid lavas of Kilauea Volcano, Hawaii: *Jour. Petrology*, v. 12, p. 1–65.
- Wright, T. L., Kinoshita, W. T., and Peck, D. L., 1968, March 1965

- eruption of Kilauea Volcano and the formation of Makaopuhi lava lake: *Jour. Geophys. Research*, v. 73, p. 3181-3205.
- Wright, T. L., Swanson, D. A., and Duffield, W. A., 1975, Chemical compositions of Kilauea east-rift lava, 1968-1971: *Jour. Petrology*, v. 16, p. 110-133.
- Wright, T. L., and Weiblen, P. W., 1968, Mineral composition and paragenesis in tholeiitic basalt from Makaopuhi lava lake, Hawaii: *Geol. Soc. America Spec. Paper* 115, p. 242-243.
- Yokoyama, Izumi, 1971, A model for the crustal deformations around volcanoes: *Jour. Physics Earth*, v. 19, p. 199-207.
- Zablocki, C. J., Tilling, R. I., Peterson, D. W., Christiansen, R. L., Keller, G. V., and Murray, J. C., 1974, A deep research drill hole at the summit of an active volcano, Kilauea, Hawaii: *Geophys. Research Letters*, v. 1, no. 7, p. 323-326.